Redox chemistry of uranium in reducing, dilute to concentrated NaCl solutions

Neşe Çevirim-Papaioannou[a,*], Ezgi Yalçıntaş[a,b], Xavier Gaona[a,**], Kathy Dardenne[a], Marcus Altmaier[a], Horst Geckeis[a]

[a] *Karlsruhe Institute of Technology, Institute for Nuclear Waste Disposal, P.O. Box 3640, 76021, Karlsruhe, Germany*
[b] *Los Alamos National Laboratory, Carlsbad, NM, 88220, USA*

ARTICLE INFO

Keywords:
Uranium
Redox
Hydrolysis
Kinetics
Thermodynamics
UO_2
Uranate

ABSTRACT

The redox behaviour of uranium was investigated in 0.1 and 5.0 M NaCl solutions at $2 \leq pH_m \leq 14.5$ ($pH_m = -\log [H^+]$) in the presence of different reducing chemical systems (Sn(II), $Na_2S_2O_4$, Sn(II) + TiO_2, Sn(II) + Fe(0), Sn(II) + Fe_3O_4). All experiments were performed under Ar atmosphere at $T = (22 \pm 2)$ °C. Uranium was added to independent batch samples as U(VI) (with $[U]_0 = 3.0 \cdot 10^{-5}$ or $4.2 \cdot 10^{-4}$ M), and the evolution of uranium concentration monitored for $t \leq 635$ days. After attaining equilibrium conditions, [U] was found in all cases clearly below the solubility of U(VI) solid phases ($UO_3 \cdot 2H_2O$(cr) or $Na_2U_2O_7 \cdot H_2O$(cr)) and in good agreement with the solubility of tetravalent UO_2(am, hyd) as calculated with available thermodynamic data. This observation is in line with (pe + pH_m) measurements, which in all cases fell in the stability field of U(IV). Solvent extraction and XANES confirmed also that uranium is predominantly found as U(IV) in the aqueous and solid phases investigated. No evidence on the formation of anionic hydrolysis species of U(IV) was obtained up to $pH_m = 14.5$. Based on our long-term redox study, we conclude that previous investigations reporting the formation of $U(OH)_5^-$ and $U(OH)_6^{2-}$ are possibly flawed by insufficient equilibration time, which prevented the complete reduction of U(VI) to U(IV). Our results further confirm that experimental pH_m and E_h values measured in buffered systems can be considered as reliable parameters to predict the redox behaviour of U in dilute to concentrated NaCl systems.

1. Introduction

Uranium is a relevant actinide for the long-term safety assessment of underground repositories for the disposal of nuclear waste due to the large inventory in spent nuclear fuel, the long half-life of U isotopes in the waste (mostly ^{238}U with $t_{1/2} = 4.47 \cdot 10^9$ years, but also ^{235}U with $t_{1/2} = 7.04 \cdot 10^8$ years and ^{236}U with $t_{1/2} = 2.34 \cdot 10^7$ years) and the formation of stable redox states (+IV and +VI) with remarkably different chemical behaviour. After the closure of a deep geological repository, reducing conditions are expected to develop due to the anoxic corrosion of iron. Water intrusion into the repository may lead to the generation of aqueous systems, whose composition is defined by the groundwater of the host-rock, the technical barriers used in the repository (*e.g.* cement) and the waste itself. This imposes a variety of boundary conditions, which range from dilute systems (in granite and most repository concepts in clay) to concentrated brines as those expected in salt-rock-based repositories (Kim and Grambow, 1999; Metz et al., 2003, 2012; Bube et al., 2013). Cementitious environments as those used for the stabilization of the waste (especially for L/ILW) and for construction purposes will buffer the pH in the hyperalkaline range ($10 \leq pH \leq 13.3$) (Wieland and Van Loon, 2002).

The thermochemical database (TDB) project of the Nuclear Energy Agency (NEA) provides the most comprehensive and authoritative selection of thermodynamic data currently available for uranium (Grenthe et al., 1992; Guillaumont et al., 2003; Hummel et al., 2005). Data selection includes thermodynamic quantities of redox reactions, solubility phenomena, hydrolysis and complexation with inorganic and organic ligands.

U(VI) shows an amphoteric behaviour and precipitates as $UO_3 \cdot 2H_2O$(cr) and M–U(VI)–OH(s) with $M = Na^+$, K^+ or Ca^{2+} (among other cations) under acidic and alkaline conditions, respectively. It hydrolyses strongly forming polymeric hydrolysis species in acidic conditions where U(VI) shows higher solubility, whereas monomeric anionic hydrolysis species dominate in near-neutral to hyperalkaline pH conditions. Based upon

* Corresponding author.
** Corresponding author.
E-mail addresses: nese.cevirim@kit.edu (N. Çevirim-Papaioannou), xavier.gaona@kit.edu (X. Gaona).

experimental studies published until 2002, the update book of the NEA–TDB (Guillaumont et al., 2003) selected equilibrium constants for the following hydrolysis species (n,m) (as $(UO_2)_n(OH)_m^{2n-m}$): (1,1), (1,2), (1,3), (1,4), (2,1), (2,2), (2,3), (3,4), (3,5), (3,7) and (4,7). In a recent publication, Altmaier and co-workers updated this thermodynamic model based on a comprehensive solubility and spectroscopic study in NaCl solutions, taking also into consideration the available data published since 2002 (Altmaier et al., 2017).

The solubility and hydrolysis of U(IV) have been far less investigated than that of U(VI), most likely due to the challenges in stabilizing the former oxidation state (especially in alkaline conditions) and to the formation of the sparingly soluble oxo-hydroxide UO_2(am, hyd). Indeed, most of the publications available in the literature on the solution chemistry of U(IV) at pH > 4 are solubility studies with UO_2(s)[1] (Gayer and Leider, 1957; Galkin and Stepanov, 1960; Tremaine et al., 1981; Ryan and Rai, 1983; Bruno et al., 1986; Parks and Pohl, 1988; Rai et al., 1990; Casas et al., 1998; Neck and Kim, 2001; Fujiwara et al., 2003, 2005). Three relevant but controversial aspects arise from these studies:

- Solubility studies with U(IV) are challenged by difficulties in solid phase characterization. U(IV) (as well as other An(IV)) tends to form amorphous oxo-hydroxide phases, whose stability can be strongly impacted by effects such as particle size, aging, degree of hydration or surface alteration (including sorption). Several of these effects are easily missed with standard characterization approaches.
- The formation of anionic hydrolysis species of U(IV) ($U(OH)_5^-$ and $U(OH)_6^{2-}$) under alkaline conditions has been proposed in some studies (Gayer and Leider, 1957; Galkin and Stepanov, 1960; Tremaine et al., 1981; Fujiwara et al., 2005) and disregarded by others (Ryan and Rai, 1983; Parks and Pohl, 1988; Neck and Kim, 2001). We note that the first volume of the NEA–TDB series (Grenthe et al., 1992) included a limiting value for $\Delta_f G^\circ_m\{U(OH)_5^-\}$ in the selected data set, which was based on the assumption that a $\{U(OH)_5^-\}$ > a$\{U(OH)_4(aq)\}$ at pH > 12.
- Several reducing systems have been used to retain uranium in +IV redox state: H_2(g), $Na_2S_2O_4$, Zn, Fe(0), $EuCl_2$, hydrazine, among others (Ryan and Rai, 1983; Bruno et al., 1986; Parks and Pohl, 1988; Casas et al., 1998; Fujiwara et al., 2003, 2005; Zhao et al., 2014). In spite of this, oxidation of U(IV) to U(VI) (especially under hyperalkaline pH conditions) was reported in some studies and suspected in some others.

A large number of experimental studies have investigated the reduction of U(VI) in the presence of magnetite and other corrosion products of Fe (Cantrell et al., 1995; Grambow et al., 1996; Fiedor et al., 1998; El Aamrani et al., 1999; Farrell et al., 1999; Liger et al., 1999a; Cui and Spahiu, 2002b; Missana et al., 2003; O'Loughlin et al., 2003; Scott et al., 2005; Duro et al., 2008; Ilton et al., 2010; Huber et al., 2012; Latta et al., 2012; Bruno et al., 2018). These studies highlight the role of surfaces in the catalysis of the reduction process, and point to a number of variables affecting the reduction kinetics such as pH, E_h, composition of the ionic media or Fe(II) content (in magnetite). We note that most of these studies target weakly acidic to weakly alkaline pH conditions, with the exception by Huber et al. (2012) and Bruno et al. (2018) covering up to pH ≈ 11 and ≈ 13, respectively.

Spahiu and co-workers investigated the redox behaviour of U(VI) in the presence of H_2(g) and carbonate, both in the absence and presence of UO_2(s) (Spahiu et al., 2000, 2004). A decrease of the initial U(VI) concentration ($\approx 8 \cdot 10^{-6}$ M) was only observed after the addition of UO_2(s) to the system. The authors concluded that H_2(g) does not reduce U(VI) carbonate species in the absence of a catalyst, but that reduction takes place in the presence of UO_2(s) surfaces. Under similar experimental conditions but in the absence of H_2(g), Cui and Spahiu reported the reduction of U(VI) by UO_2(s) and proposed the formation of a layer of UO_{2+x} on fresh UO_2(s) surfaces (Cui and Spahiu, 2002a).

The summary above highlights that relevant uncertainties still exist with regard to the solubility and hydrolysis of uranium. These uncertainties mostly affect U(IV), but translate also to ill-defined redox boundaries with U(VI), especially under alkaline conditions. In this context, our study aims at (i) investigating the reduction of U(VI) to U(IV) in a range of reducing systems covering $2 \le pH_m \le 14.5$, but with special focus to alkaline to hyperalkaline conditions; (ii) evaluating the impact of high salinity (as 5.0 M NaCl) on the redox chemistry of uranium; (iii) studying the reduction kinetics defined by different reducing systems; (iv) assessing the formation of anionic hydrolysis species of U(IV) under hyperalkaline pH conditions; and (v) contrasting newly generated experimental data with thermodynamics calculations, and contributing (whenever possible) to reducing existing uncertainties. The redox experiments designed for this purpose start from oversaturated U(VI) solutions, and consider differences in solubility between U(VI) and U(IV) solid phases as main criteria to probe the reduction to U(IV). Considering the relevance of kinetics described in previous investigations, very long equilibration times ($t \le 635$ days) have been allowed for these systems. Because of the known role of (given) surfaces in catalysing redox reactions, a series of experiments were performed in the presence of TiO_2, Fe(0) and Fe_3O_4(cr). Titanium dioxide is a well-known and widely used photocatalyst, whereas Fe(0) and Fe_3O_4(cr) are very relevant solid phases in the context of nuclear waste disposal, also with known reducing properties. For selected solid and aqueous samples, the redox state of uranium is determined using solvent extraction and XANES techniques. Further insights on the U(VI) / U(IV) redox boundaries are gained by comparing systematic pH_m and E_h measurements with calculations performed using thermodynamic data available in the literature.

2. Thermodynamic background

Data selected in the update book of the NEA–TDB (Guillaumont et al., 2003) are taken as basis for the thermodynamic model considered in this study. Thermodynamic data selected in the NEA–TDB for U(VI) are updated with the recent study by Altmaier et al. (2017), where both solubility and hydrolysis were systematically investigated over a large range of ionic strength. NEA–TDB data selection for U(IV) is complemented with the comprehensive review work by Neck and Kim (2001) on An(IV) solubility and hydrolysis. Although most of the thermodynamic data reported by these authors are consistent with the NEA–TDB selection, Neck and Kim provide equilibrium constants for the second and third hydrolysis species of U(IV), currently not selected in the NEA–TDB. Equilibrium constants considered in the thermodynamic calculations in this study (*Pourbaix* diagrams and solubility curves) are summarized in Table 1. The combination of U(VI) and U(IV) solubility and hydrolysis constants summarized in the table provides a clear insight on the ill-defined redox borderline for the couple U(VI) / U(IV) in alkaline conditions. We note that uncertainties in the equilibrium constants of the key redox reactions (1)–(3) are very large and range from ± 1.0 to ± 1.5.

Main redox reactions in aqueous phase (pH > 8)

$$UO_2(OH)_3^- + 3\,H^+ + 2\,e^- \leftrightarrow U(OH)_4(aq) + H_2O(l) \quad (1)$$

$$\log {}^*K^\circ = (19.7 \pm 1.5)$$

$$UO_2(OH)_4^{2-} + 4\,H^+ + 2\,e^- \leftrightarrow U(OH)_4(aq) + 2\,H_2O(l) \quad (2)$$

$$\log {}^*K^\circ = (30.9 \pm 1.4)$$

Main redox reaction in solid phase (pH > 8, $[Na^+]$ > 0.01 M)

$$0.5\,Na_2U_2O_7{\cdot}H_2O(cr) + 2\,e^- + 3\,H^+ \leftrightarrow UO_2(am, hyd) + Na^+ + 2\,H_2O(l) \quad (3)$$

[1] We use here a generic notation for solids, (s). This accounts for the different degrees of crystallinity of the solids used in the solubility experiments, ranging from amorphous to crystalline and very likely including also colloidal phases.

Table 1
Equilibrium constants for redox, solubility and hydrolysis reactions of uranium considered for thermodynamic calculations in the present study.

Reaction	log *K°	Reference
Redox		
$U^{4+} + e^- \leftrightarrow U^{3+}$	–(9.353 ± 0.07)	Guillaumont et al. (2003)
$UO_2^{2+} + 4\ H^+ + 2e^- \leftrightarrow U^{4+} + 2\ H_2O(l)$	(9.04 ± 0.04)	Guillaumont et al. (2003)
$UO_2^{2+} + e^- \leftrightarrow UO_2^+$	(1.49 ± 0.02)	Guillaumont et al. (2003)
Solubility		
$UO_2(am, hyd) + 4\ H^+ \leftrightarrow U^{4+} + 4\ H_2O(l)$	(1.50 ± 1.00)	Guillaumont et al. (2003)
$UO_3{\cdot}2H_2O(cr) + 2\ H^+ \leftrightarrow UO_2^{2+} + 3\ H_2O(l)$	(5.35 ± 0.13)	Altmaier et al. (2017)
$0.5\ Na_2U_2O_7{\cdot}H_2O(cr) + 3\ H^+ \leftrightarrow Na^+ + UO_2^{2+} + 2\ H_2O(l)$	(12.20 ± 0.20)	Altmaier et al. (2017)
U(IV) hydrolysis		
$U^{4+} + H_2O(l) \leftrightarrow UOH^{3+} + H^+$	–(0.40 ± 0.20)	Neck and Kim (2001)
$U^{4+} + 2\ H_2O(l) \leftrightarrow U(OH)_2^{2+} + 2\ H^+$	–(1.10 ± 1.00)	Neck and Kim (2001)
$U^{4+} + 3\ H_2O(l) \leftrightarrow U(OH)_3^+ + 3\ H^+$	–(4.70 ± 1.00)	Neck and Kim (2001)
$U^{4+} + 4\ H_2O(l) \leftrightarrow U(OH)_4(aq) + 4\ H^+$	–(10.00 ± 1.40)	Neck and Kim (2001); Guillaumont et al. (2003)
U(VI) hydrolysis		
$UO_2^{2+} + H_2O(l) \leftrightarrow UO_2OH^+ + H^+$	–(5.25 ± 0.24)	Guillaumont et al. (2003)
$UO_2^{2+} + 2\ H_2O(l) \leftrightarrow UO_2(OH)_2(aq) + 2\ H^+$	–(12.15 ± 0.17)	Guillaumont et al. (2003)
$UO_2^{2+} + 3\ H_2O(l) \leftrightarrow UO_2(OH)_3^- + 3\ H^+$	–(20.70 ± 0.42)	Altmaier et al. (2017)
$UO_2^{2+} + 4\ H_2O(l) \leftrightarrow UO_2(OH)_4^{2-} + 4\ H^+$	–(31.90 ± 0.33)	Altmaier et al. (2017)
$2\ UO_2^{2+} + 2\ H_2O(l) \leftrightarrow (UO_2)_2(OH)_2^{2+} + 2\ H^+$	–(5.62 ± 0.06)	Guillaumont et al. (2003)
$3\ UO_2^{2+} + 4\ H_2O(l) \leftrightarrow (UO_2)_3(OH)_4^{2+} + 4\ H^+$	–(11.90 ± 0.30)	Guillaumont et al. (2003)
$3\ UO_2^{2+} + 5\ H_2O(l) \leftrightarrow (UO_2)_3(OH)_5^+ + 4\ H^+$	–(15.55 ± 0.12)	Guillaumont et al. (2003)
$3\ UO_2^{2+} + 7\ H_2O(l) \leftrightarrow (UO_2)_3(OH)_7^- + 7\ H^+$	–(32.20 ± 0.80)	Guillaumont et al. (2003)
$4\ UO_2^{2+} + 7\ H_2O(l) \leftrightarrow (UO_2)_4(OH)_7^+ + 7\ H^+$	–(21.90 ± 1.00)	Guillaumont et al. (2003)

$$\log {}^*K^\circ = (19.7 \pm 1.0)$$

The specific ion interaction theory (SIT) (Ciavatta, 1980) is the method adopted by the NEA–TDB (Grenthe et al., 1992; Guillaumont et al., 2003) for the correction of ion interaction processes. The basic formulism in SIT considers:

$$\log \gamma_j = z_j^2\ D + \Sigma_k \varepsilon(j, k, I_m)\ m_k \quad (4)$$

with

$$D = \frac{A\sqrt{I_m}}{1 + Ba_j\sqrt{I_m}} \quad (5)$$

where z_j is the charge of the ion j, D is the Debye-Hückel term, m_k is the molality of the oppositely charged ion k, and $\varepsilon(j, k, I_m)$ is the specific ion interaction parameter. A and B in the Debye-Hückel terms are constants which are temperature and pressure dependent, whereas a_j is an ion size parameter for the hydrated ion j. At 25 °C and 1 bar, the terms A and Ba_j have a value of 0.509 $kg^{0.5}{\cdot}mol^{-0.5}$ and 1.5 $kg^{0.5}{\cdot}mol^{-0.5}$, respectively. SIT ion interaction coefficients used in the present work for activity corrections are summarized in Table 2.

3. Experimental

3.1. Chemicals

Sodium chloride (NaCl, EMSURE®), sodium hydroxide (NaOH, Titrisol®), hydrochloric acid (HCl, Titrisol®), nitric acid (HNO_3, SUPRAPUR), sodium dithionite ($Na_2S_2O_4$, ≥87%), titanium dioxide (TiO_2 rutile, ≥ 99.5%), metallic iron powder (≥99.5%, grain size 10 μm) and xylene (≥97.5%) were obtained from Merck. $SnCl_2$ (98%), MES (2-(N-morpholino)ethanesulfonic acid, ≥ 99.5%; $pK_a^\circ = 6.15$) and TRIS (2-Amino-2-(hydroxymethyl)propane-1,3-diol, ≥ 99.5%; $pK_a^\circ = 8.3$) were purchased from Sigma Aldrich. PMBP (1-phenyl-3-methyl-4-benzoyl-2-pyrazolin-5-on, ≥ 99.0%) was provided by Fluka. Magnetite (α-Fe_3O_4(cr), 60–120 nm) was prepared hydrothermally at KIT–INE following the protocol previously described in the literature (Schwertmann and Cornell, 2000).

All solutions were prepared with ultrapure water purified with a Milli-Q-academic (Millipore) apparatus and purged with Ar before use. All sample preparation and handling was performed in an Ar-glove box (< 1 ppm O_2) at $T = (22 \pm 2)$ °C.

Table 2
SIT ion interaction coefficients (in $kg{\cdot}mol^{-1}$) of U(IV), U(V) and U(VI) aquaions and hydrolysis species in NaCl media at 25 °C considered for activity corrections in the present study.

I	J	$\varepsilon(i,j)$	Reference
U(III) species			
U^{3+}	Cl^-	(0.18 ± 0.05)[a]	Guillaumont et al. (2003)
U(IV) species			
U^{4+}	Cl^-	(0.36 ± 0.10)	Neck and Kim (2001)
$U(OH)^{3+}$	Cl^-	(0.20 ± 0.10)	Neck and Kim (2001)
$U(OH)_2^{2+}$	Cl^-	(0.10 ± 0.10)	Neck and Kim (2001)
$U(OH)_3^+$	Cl^-	(0.05 ± 0.10)	Neck and Kim (2001)
$U(OH)_4(aq)$	Na^+, Cl^-	0	b
U(V) species			
UO_2^+	Cl^-	(0.09 ± 0.05)[a]	Guillaumont et al. (2003)
U(VI) species			
UO_2^{2+}	Cl^-	(0.21 ± 0.02)	Altmaier et al. (2017)
$UO_2(OH)^+$	Cl^-	(0.10 ± 0.10)	Altmaier et al. (2017)
$UO_2(OH)_2(aq)$	Na^+, Cl^-	0	b
$UO_2(OH)_3^-$	Na^+	–(0.24 ± 0.09)	Altmaier et al. (2017)
$UO_2(OH)_4^{2-}$	Na^+	(0.01 ± 0.04)	Altmaier et al. (2017)
$(UO_2)_2(OH)_2^{2+}$	Cl^-	(0.30 ± 0.06)	Altmaier et al. (2017)
$(UO_2)_3(OH)_4^{2+}$	Cl^-	–(0.07 ± 0.17)	Altmaier et al. (2017)
$(UO_2)_3(OH)_5^+$	Cl^-	(0.24 ± 0.15)	Altmaier et al. (2017)
$(UO_2)_3(OH)_7^-$	Na^+	–(0.24 ± 0.09)	Altmaier et al. (2017)
$(UO_2)_4(OH)_7^+$	Cl^-	(0.17 ± 0.18)	Altmaier et al. (2017)

a. Estimated considering $\varepsilon(M^{z+}, Cl^-) = 0.38{\cdot}\varepsilon(M^{z+}, ClO_4^-) \pm 0.1\ kg\ mol^{-1}$ (Fuger et al., 2008); b. by definition in SIT.

3.2. pH_m and E_h measurements

The hydrogen ion concentration ($pH_m = -\log [H^+]$, in molal units) was measured using combination pH electrodes (ROSS, Orion) calibrated with standard pH buffers (pH 1–12, Merck). Experimentally measured pH_{exp} values were corrected with empirical "A_m" factors to obtain pH_m ($pH_m = pH_{exp} + A_m$). Such corrections are required in solutions of ionic strength $I \geq 0.1\ mol{\cdot}kg^{-1}$, where pH_{exp} is an operational value significantly deviating from pH. A_m-factors entail both the liquid junction potential of the electrode and the activity coefficient of H^+ at a given background electrolyte concentration. A_m-factors reported in literature for NaCl systems were used for the determination of pH_m (Altmaier et al., 2003). In NaCl–NaOH solutions with $[OH^-] > 0.03$ M, $[H^+]$ was calculated from the given $[OH^-]$ and the

conditional ion product of water.

Redox potentials were measured with Pt combination electrodes with Ag/AgCl reference system (Metrohm). The measured potentials were converted to E_h (*versus* standard hydrogen electrode, SHE) by correcting for the potential of the Ag/AgCl inner-reference electrode with 3 M KCl and T = 22 °C (+207 mV). Stable E_h readings were normally obtained within 10–30 min. The apparent electron activity ($pe = -\log a_{e^-}$) was calculated from $E_h = -(RT/F) \ln a_{e^-}$, according to the relation $pe = 16.9\ E_h$ (V).

3.3. Preparation and characterization of redox samples

Oversaturation experiments with U(VI) were performed in 0.1 M and 5.0 M NaCl solutions with $2 \le pH_m \le 14.5$. Inactive solutions (without uranium) were pre-equilibrated in independent batch samples with the following reducing systems: Sn(II)[2], $Na_2S_2O_4$, Sn(II) + TiO_2, Sn(II) + Fe(0) and Sn(II) + Fe_3O_4(cr). The pH_m values were adjusted using HCl–NaCl and NaCl–NaOH solutions with I = 0.1 or 5.0 M. MES (5 mM) and TRIS buffers (1 mM) were used to fix the pH_m at 6 and 8, respectively. Two different initial uranium concentrations were used in the experiments: $[U(VI)]_0 = 4.2{\cdot}10^{-4}$ and $3{\cdot}10^{-5}$ M. Table 3 provides a detailed summary of the experimental conditions used in this study.

The concentration of uranium was quantified at regular time intervals (up to 635 days) after phase separation by ultrafiltration (10 kD filters Nanosep® and Mikrosep®, Pall Life Sciences; 2–3 nm cut-off). Aliquots of the original samples were diluted in 2% HNO_3 in 5 ml screw-cap tubes (100–5000 dilution factor, depending upon NaCl and uranium concentration) and measured using ICP-MS (Perkin Elmer ELAN 6100). Measurement of blank samples normally resulted in 0.001–0.002 ppb U, leading to detection limits of $\approx 10^{-7}$ to $\approx 10^{-11}$ M (depending upon dilution factor), as calculated considering 3σ of the blank.

After attaining equilibrium conditions (constant pH_m, E_h and [U] measurements), a solvent extraction approach was used to determine the oxidation state of U in the aqueous phase of samples containing $[U] \ge 10^{-5}$ M (Coronel et al., 1982; Fellhauer, 2013). 250 µL of the supernatant solution of selected samples were acidified with 250 µL of 2 M HCl after ultrafiltration with 10 kD filters. Acidified samples were contacted with 500 µL xylene containing 0.025 M PMBP. The mixture was vigorously shaken for 3–5 min and centrifuged at 12000 g for 5 min to separate organic and aqueous phases. The concentration of uranium in the aqueous phase was quantified by ICP-MS and attributed to presence of U(VI).

3.4. XANES measurements

Uranium L_{III}-edge X-ray absorption near-edge structure (XANES) spectra were recorded at the INE-Beamline and ACT-Beamline at KIT Synchrotron (formerly ANKA), KIT Campus North, in Karlsruhe, Germany (Rothe et al., 2012; Zimina et al., 2017). Both solid (INE-beamline) and aqueous (ACT-Beamline) phases were characterized to determine the redox state of U. Three samples were investigated: (i) supernatant of the sample containing 20 mM Sn(II) in 0.1 M NaCl at pH_m = 2.2, (ii) solid phase of the sample equilibrated in 20 mM Sn(II) + 15 mg Fe(0) in 0.1 M NaCl at pH_m = 10.9 (iii) solid phase of the sample equilibrated in 20 mM Sn(II) in 5.0 M NaCl at pH_m = 11.9. U(IV) and U(VI) standards (both aqueous and solids) were prepared for the identification of the redox state of uranium in the unknown samples. A nitrate-free 0.01 M U(VI) stock solution was prepared in 1.0 M HCl after a series of dissolution / precipitation steps with $UO_2(NO_3)_2$ in HCl / NaOH. A solid $Na_2U_2O_7{\cdot}H_2O$(cr) synthesized in our previous study (Altmaier et al., 2017) was contacted with a $pH_m \approx 12$ solution and used as a reference for U(VI) solid phases. A 0.01 M U(IV) stock solution was prepared by electrolysis of the U(VI) stock in 1.0 M HCl. The redox purity of the resulting solution was confirmed by UV-vis (see Supporting Information). A fraction of the U(IV) stock solution was precipitated in a $pH_m \approx 12$ solution containing $Na_2S_2O_4$ as holding reducing agent. The resulting UO_2(am, hyd) solid was aged for ≈ 2 months and used as reference for U(IV) solid phases in the XANES measurements.

In all cases, approximately 300 µL of the suspension were transferred to a 400 µL polyethylene vial under an Ar atmosphere and centrifuged at 4020*g* for 10 min to obtain a compacted solid phase at the bottom of the vial. The vials were mounted in a gas-tight cell with windows of Kapton® film (polyimide) inside the Ar-glovebox and transported to ANKA. The measurements were conducted within a few hours after sample preparation.

Uranium L_{III}-edge (17166 eV) XANES spectra (7–9 replicates per sample) were collected at room temperature under a continuous flow of Ar. The INE-Beamline is equipped with a Ge(422) double crystal monochromator (DCM) coupled with a collimating and a focusing Rh coated mirrors before and after the DCM, respectively. The DCM-crystals were detuned at 70%. The ACT-Beamline is equipped for these measurements with Si(111) double crystal monochromator (DCM) coupled with a collimating and a focusing Rh coated mirrors before and after the DCM, respectively. At both beamlines, the beam spotsize on the sample is below 1 mm diameter. The energy calibration was performed by assigning the energy of 17038 eV to the first inflection point of the K-edge absorption spectrum of the Y metal foil. The incident and transmitted beam intensities were measured by argon-filled ionization chambers. XANES data reduction and analysis were performed with the ATHENA software of the Demeter 0.9.26 package following standard procedures (Ravel and Newville, 2005).

Table 3
Experimental conditions used in this study for the investigation of uranium redox behaviour under reducing conditions.

Background Electrolyte	Reducing system	$[U(VI)]_0$	pH_m range	Contact time [days]
0.1 M NaCl	2 mM Sn(II)	$4.2{\cdot}10^{-4}$ M	12.8	≤625
0.1 M NaCl	10 mM Sn(II)	$4.2{\cdot}10^{-4}$ M	12–12.8	≤238
0.1 M NaCl	20 mM Sn(II)	$3.0{\cdot}10^{-5}$ M	2–12.8	≤574
0.1 M NaCl	20 mM Sn(II) + 10 mg TiO_2	$3.0{\cdot}10^{-5}$ M	2–12.8	≤574
0.1 M NaCl	20 mM Sn(II) + 10 mg Fe_3O_4(cr)	$3.0{\cdot}10^{-5}$ M	8–12.8	≤574
0.1 M NaCl	20 mM Sn(II) + 15 mg Fe(0)	$3.0{\cdot}10^{-5}$ M	8–12.8	≤574
0.1 M NaCl	20 mM $Na_2S_2O_4$	$3.0{\cdot}10^{-5}$ M	10.8–12.8	≤177
5.0 M NaCl	20 mM Sn(II)	$3.0{\cdot}10^{-5}$ M	3.5–14.5	≤178

4. Results and discussion

The redox behaviour and solubility of uranium are discussed in the following sections as classified by reducing system: Sn(II), $Na_2S_2O_4$, Sn(II) + TiO_2, Sn(II) + Fe(0) and Sn(II) + Fe_3O_4(cr). Experimentally measured E_h and pH_m values are plotted in *Pourbaix* diagrams calculated for 0.1 M or 5.0 M NaCl using the thermodynamic and activity models summarized in Section 2. *Pourbaix* diagrams are prepared with the code Medusa developed by Ignasi Puigdomènech (Puigdomènech, 1983) using the above data selection. For each reducing system, the concentration of U determined at

[2] Sn(II) forms sparingly soluble oxo-hydroxides that show an amphoteric behaviour (formation of cationic and anionic hydrolysis species in acidic and alkaline pH conditions, respectively). The presence of Sn(II) solid phase/s (possibly $Sn(OH)_2$(s) and / or $Sn_6O_4(OH)_4$(s)) was observed in all samples with $5 < pH_m < 12$. For these samples, the total concentration of Sn(II) in solution was clearly below than the original [Sn(II)], although [Sn] was not quantified experimentally.

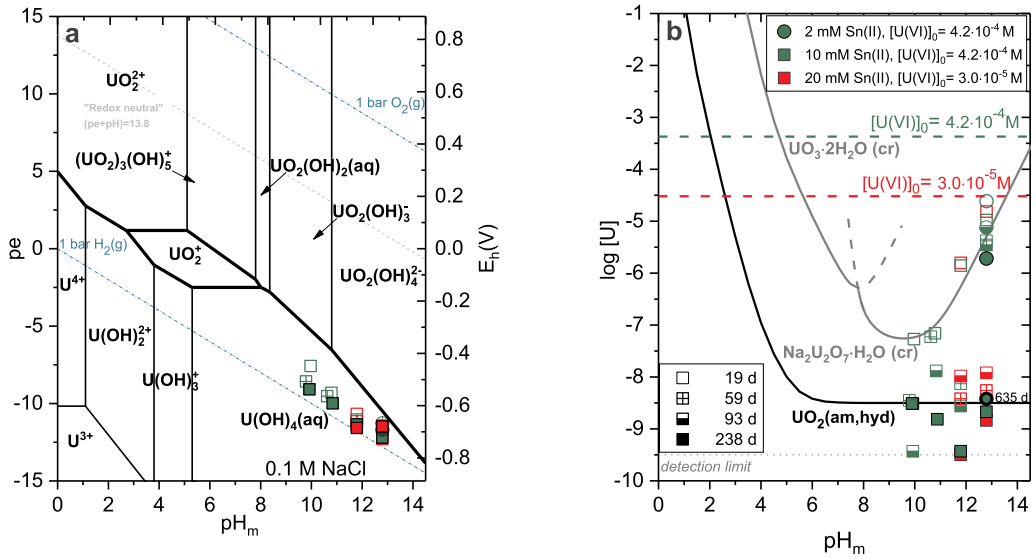

Fig. 1. a. Pourbaix diagram of uranium calculated for [U] = 3.0·10^{-5} M and 0.1 M NaCl (minor differences observed for calculations using 4.2·10^{-4} M). Calculations performed allowing the precipitation of $UO_3·2H_2O$(cr), $Na_2U_2O_7·H_2O$(cr) and UO_2(am, hyd). Symbols represent experimentally measured E_h and pH_m values in 0.1 M NaCl systems containing 2, 10 and 20 mM Sn(II); b. concentrations of uranium measured after 10 kD ultrafiltration for 0.1 M NaCl systems with [Sn(II)] = 2, 10 and 20 mM, and $[U(VI)]_0$ = 4.2·10^{-4} and 3.0·10^{-5} M. Solid lines correspond to solubility curves of $UO_3·2H_2O$(cr), $Na_2U_2O_7·H_2O$(cr) and UO_2(am, hyd) calculated using thermodynamic data in Section 2. Dashed horizontal lines indicate the initial U(VI) concentrations in the experiments. The different filling of the data points refers to the different equilibration times.

$9 \le t$ [days] ≤ 635 is plotted as a function of pH_m, and compared with the solubility calculated for the main U(VI) ($UO_3·2H_2O$(cr) and $Na_2U_2O_7·H_2O$(cr)) and U(IV) (UO_2(am, hyd)) solid phases expected to form in the conditions of our study. The difference in solubility between U(VI) and U(IV) solid phases is used as main criterion to assess the reduction of U(VI) to U(IV) behaviour in neutral to alkaline pH region, and complemented in specific cases with solvent extraction and XANES techniques.

4.1. Redox behaviour and solubility of uranium in reducing systems

4.1.1. Sn(II) systems in 0.1 and 5.0 M NaCl

In Fig. 1a., the E_h and pH_m values measured in 0.1 M NaCl systems containing 2, 10 and 20 mM Sn(II) are shown. Experimental E_h and pH_m values are plotted in a *Pourbaix* diagram of uranium calculated for the same boundary conditions and $[U]_{tot}$ = 3.0·10^{-5} M. The figure shows that Sn(II) sets very strongly reducing conditions, in all cases well below the calculated U(VI/IV) borderline. This suggests that U(VI) should reduce to U(IV) in the course of the experiment. Fig. 1a also shows that E_h values remain stable within the timeframe considered for this system (t = 238 days).

Fig. 1b shows the concentrations of uranium measured in this system after 10 kD ultrafiltration. Different shapes and colours of symbols correspond to the different concentrations of Sn(II) (2, 10 and 20 mM) and (initial) U(VI) (4.2·10^{-4} and 3.0·10^{-5} M). The figure also shows the solubility of U(VI) and U(IV) solid phases calculated for 0.1 M NaCl systems and according to thermodynamic data summarized in Section 2.

A very significant decrease of uranium concentration (down to 10^{-8} – 10^{-9} M) is observed in all investigated Sn(II) systems, which suggests the complete reduction of U(VI) to U(IV) and a solubility-control by UO_2(am, hyd). However, reduction kinetics are strongly affected by $[U(VI)]_0$, [Sn(II)] and pH_m:

- The fastest reduction (≈ 59 days) is observed for those samples with highest Sn(II) concentration (20 mM) and lowest $[U(VI)]_0$ (3.0·10^{-5} M).
- Those samples with $[U(VI)]_0$ = 4.2·10^{-4} M and [Sn(II)] = 10 mM show pH_m-dependent reduction kinetics. Hence, fast reduction (≈59 days) is observed within $10 \le pH_m \le 12$, whereas significantly longer contact time (≈ 238 days) is required to reduce U(VI) to U(IV) at pH_m = 12.8. Such behaviour can be rationalized by the decreased driving force for the reduction of U(VI) to U(VI): Δpe (as $|pe_{exp} - pe_{borderline}|$) becomes smaller with increasing pH_m (Fellhauer, 2013; Kobayashi et al., 2013) (see Fig. 1a.).
- The sample with $[U(VI)]_0$ = 4.2·10^{-4} M, [Sn(II)] = 2 mM and pH_m = 12.8 shows the slowest reduction kinetics. A first, fast drop in uranium concentration is produced within 19 days leading to [U] ≈ 10^{-5} M, in excellent agreement with a solubility control by $Na_2U_2O_7·H_2O$(cr). This concentration of uranium is retained in solution up to ≈ 238 days. A much longer contact time (635 days, black circle in Fig. 1b.) is required to decrease uranium concentration down to 10^{-8} – 10^{-9} M, which corresponds to the complete reduction of U(VI) to U(IV). Very likely both $Na_2U_2O_7·H_2O$(cr) and UO_2(am, hyd) solid phases co-exist for a long time until the solid phase transformation is completed, but in such cases the solubility is controlled by the more soluble phase.

An additional series of samples in the presence of Sn(II) was prepared in 0.1 M NaCl covering a broader pH_m-range, $2 \le pH_m \le 12.8$. Independent batch experiments were prepared with 20 mM Sn(II) and $[U(VI)]_0$ = 3·10^{-5} M, conditions in which (based upon our previous experiments in alkaline pH_m conditions) a faster reduction of U(VI) to U(IV) is expected. Fig. 2a shows that Sn(II) provides very reducing conditions ($pe + pH_m = 2 \pm 1$) over the complete pH_m-range investigated, in excellent agreement with previous redox investigations using Sn(II) as reducing chemical (Kobayashi et al., 2013; Yalcintas et al., 2015). Under these boundary conditions, the reduction of U(VI) to U(IV) is completed within $t \le 177$ days for all investigated samples except the one at pH_m = 5.9 for which significantly longer contact time ($t \approx 574$ days) is required (see Fig. 2b.). The reason for the longer equilibration time required for this specific case remains unexplained, but might be related with the greater stability field of U(V) at this pH_m. The shape of the solubility curve of U obtained within $2 \le pH_m \le 12.8$ is in excellent agreement with thermodynamic calculations performed for U(IV) according to thermodynamic and activity models summarized in Section 2. This observation strongly suggests that equilibrium conditions have been attained in the system, as well as hinting towards the expected predominance of UO_2(am, hyd) as solubility controlling solid

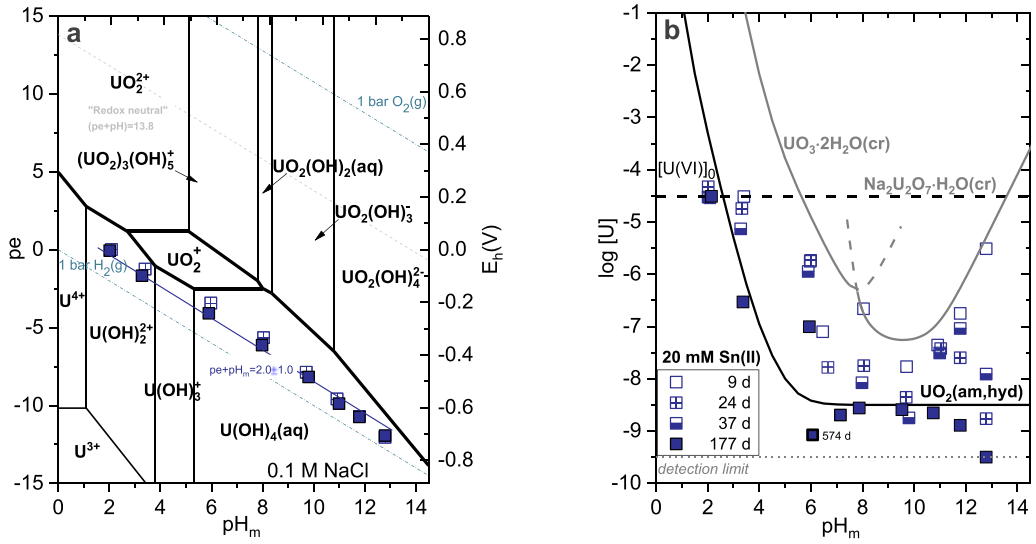

Fig. 2. a. Pourbaix diagram of uranium calculated for [U] = $3.0{\cdot}10^{-5}$ M and 0.1 M NaCl. Calculations performed allowing the precipitation of $UO_3{\cdot}2H_2O$(cr), $Na_2U_2O_7{\cdot}H_2O$(cr) and UO_2(am, hyd). Symbols represent experimentally measured E_h and pH_m values in 0.1 M NaCl systems containing 20 mM Sn(II); b. concentrations of uranium measured after 10 kD ultrafiltration for 0.1 M NaCl systems with [Sn(II)] = 20 mM and $[U(VI)]_0 = 3.0{\cdot}10^{-5}$ M. Solid lines correspond to solubility curves of $UO_3{\cdot}2H_2O$(cr), $Na_2U_2O_7{\cdot}H_2O$(cr) and UO_2(am, hyd) calculated using thermodynamic data in Section 2. Dashed horizontal line indicates the initial U(VI) concentration in the experiments. The different filling of the data points refers to the different equilibration times.

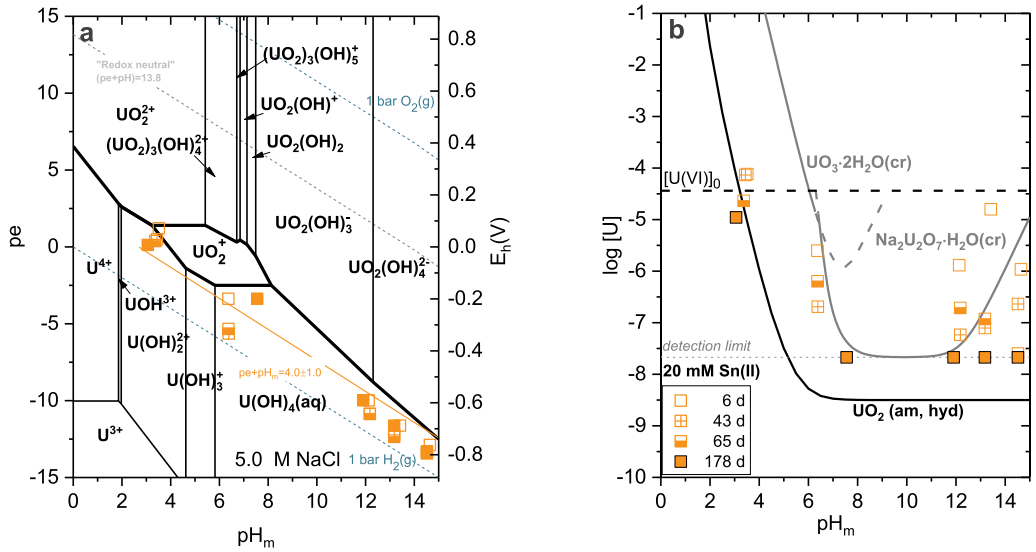

Fig. 3. a. Pourbaix diagram of uranium calculated for [U] = $3.0{\cdot}10^{-5}$ M and 5.0 M NaCl. Calculations performed allowing the precipitation of $UO_3{\cdot}2H_2O$(cr), $Na_2U_2O_7{\cdot}H_2O$(cr) and UO_2(am, hyd). Symbols represent experimentally measured E_h and pH_m values in 5.0 M NaCl systems containing 20 mM Sn(II)[3]; b. concentrations of uranium measured after 10 kD ultrafiltration for 5.0 M NaCl systems with [Sn(II)] = 20 mM and $[U(VI)]_0 = 3.0{\cdot}10^{-5}$ M. Solid lines correspond to solubility curves of $UO_3{\cdot}2H_2O$(cr), $Na_2U_2O_7{\cdot}H_2O$(cr) and UO_2(am, hyd) calculated using thermodynamic data in Section 2. Dashed horizontal line indicates the initial U(VI) concentration in the experiments. The different filling of the data points refers to the different equilibration times.

phase in equilibrium with $U(OH)_2^{2+}$, $U(OH)_3^{+}$ and $U(OH)_4$(aq) hydrolysis species.

The impact of high salinity on the redox behaviour of uranium was investigated in 5.0 M NaCl systems with $4 \leq pH_m \leq 14.5$. Independent batch samples were prepared with 20 mM Sn(II) and $[U(VI)]_0 = 3{\cdot}10^{-5}$ M. Fig. 3a shows the *Pourbaix* diagram of uranium calculated for these boundary conditions, including experimental E_h and pH_m values measured within $t \leq 178$ days. The figure shows that the Sn(II/IV) redox couple is impacted by ionic strength, leading to slightly less reducing conditions with $(pe + pH_m) = (4 \pm 1)$. In spite of this, all investigated samples are within the stability field of U(IV). Note that a similar impact of ionic strength on $(pe + pH_m)$ values was previously reported by Yalcintas et al. (2015) for Sn(II) systems in 5.0 M NaCl. Fig. 3b shows the concentrations of uranium measured in this system after 10 kD ultrafiltration, together with the solubility curves of $UO_3{\cdot}2H_2O$(cr), $Na_2U_2O_7{\cdot}H_2O$(cr) and UO_2(am, hyd) calculated for 5.0 M NaCl solutions according with thermodynamic data summarized in Section 2. The figure shows a slight decrease of uranium concentration at $pH_m \approx 4$, consistently with the reduction of U(VI) to U(IV) and a solubility-control by UO_2(am, hyd). Concentrations of U measured in near-neutral to hyper-alkaline pH_m conditions after 178 days are below the

[3] No U(VI)- and U(IV)-chloro complexes are included in these calculations. Altmaier et al. (2017) disregarded the definition of U(VI)-chloro complexes – such interaction was instead accounted for in the reported SIT coefficients. The complex UCl^{3+} was selected by Guillaumont et al. (2003), although no SIT coefficient was reported for the interaction of this cation with Cl^-. Disregarding this complex in 5.0 M NaCl systems has only a minor impact in thermodynamic calculations at pH_m below ≈ 4.

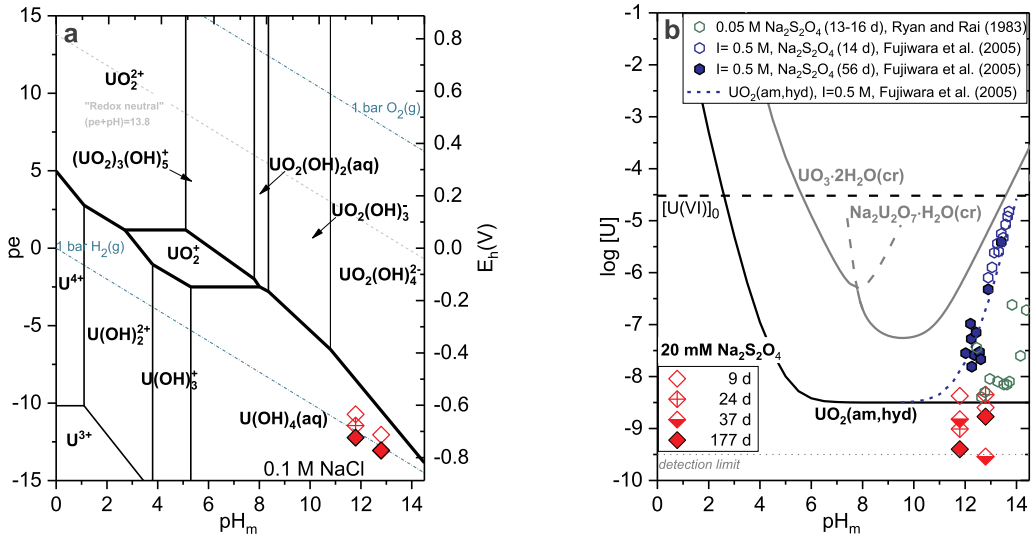

Fig. 4. a. Pourbaix diagram of uranium calculated for [U] = $3.0{\cdot}10^{-5}$ M and 0.1 M NaCl. Calculations performed allowing the precipitation of $UO_3{\cdot}2H_2O$(cr), $Na_2U_2O_7{\cdot}H_2O$(cr) and UO_2(am, hyd). Symbols represent experimentally measured E_h and pH_m values in 0.1 M NaCl systems containing 20 mM $Na_2S_2O_4$; b. red diamonds: concentrations of uranium measured in this work after 10 kD ultrafiltration for 0.1 M NaCl systems with [$Na_2S_2O_4$] = 20 mM and $[U(VI)]_0 = 3.0{\cdot}10^{-5}$ M; blue / green hexagon: solubility data reported in Fujiwara et al. (2005) and Ryan and Rai (1983), respectively. Solid lines correspond to solubility curves of $UO_3{\cdot}2H_2O$(cr), $Na_2U_2O_7{\cdot}H_2O$(cr) and UO_2(am, hyd) calculated using thermodynamic data in Section 2. Dashed blue solubility line corresponds to the solubility of UO_2(am, hyd) at I = 0.5 M calculated including the formation of $U^{IV}(OH)_5^-$ and $U^{IV}(OH)_6^{2-}$ as reported by Fujiwara et al. (2005). Dashed horizontal line indicates the initial U(VI) concentration in the experiments. The different filling of the data points refers to the different equilibration times. (For interpretation of the references to colour in this figure legend, the reader is referred to the Web version of this article.)

detection limit of ICP–MS ($\approx 10^{-7.6}$ M for this NaCl concentration). Due to the high detection limit and the low solubility of $Na_2U_2O_7{\cdot}H_2O$(cr) in 5.0 M NaCl solutions with pH_m = 7.6 and 11.9, these results do not provide conclusive insight on the redox behaviour of uranium within this pH_m-range. However, based upon measured (pe + pH_m) values and the solubility behaviour of uranium in acidic and hyperalkaline conditions, the reduction of U(VI) to U(IV) is to be expected also in these conditions. The decrease of uranium concentration observed at pH_m = 13.2 and 14.5 is consistent with the reduction of U(VI) to U(IV) and a solubility-control by UO_2(am, hyd). The solubility of U(VI) calculated for the reaction $0.5Na_2U_2O_7{\cdot}H_2O(cr) + 2H_2O(l) = UO_2(OH)_4^{2-} + Na^+ + H^+$ is 1–3 orders of magnitude greater than the experimentally measured [U] (see Fig. 3b.), thus providing conclusive evidence that U(VI) does not control the solubility of uranium under these boundary conditions.

The formation of anionic hydrolysis species of U(IV) ($U^{IV}(OH)_5^-$ and $U^{IV}(OH)_6^{2-}$) was proposed in a previous study based upon solubility experiments with the in-situ reduction of U(VI) by $Na_2S_2O_4$ (Fujiwara et al., 2005) (see discussion in Introduction and in Section 4.1.2). We note that our solubility data up to pH_m = 14.5 does not support the formation of such anionic hydrolysis species of U(IV) in significant proportions.

4.1.2. $Na_2S_2O_4$ systems in 0.1 M NaCl

The redox behaviour of uranium in the presence of 20 mM $Na_2S_2O_4$ in 0.1 M NaCl solutions with $pH_m \geq 11$ is shown in Fig. 4. $Na_2S_2O_4$ is a strong reducing agent that sets pe values at the border of water reduction (pe + pH_m) ≈ 0 (Fig. 4a.). A fast decrease in uranium concentration to [U] ≈ 10^{-9} M was observed within 9 days for all investigated samples (Fig. 4b.). This observation indicates the reduction of U(VI) to U(IV) and a solubility control by UO_2(am, hyd), in excellent agreement with thermodynamic calculations.

Fujiwara et al. (2005) conducted similar redox experiments with uranium in the presence of $Na_2S_2O_4$. As in our study, Fujiwara and co-workers started their experiments with oversaturated U(VI) solutions (alkaline 0.5, 1.0 and 2.0 M $NaClO_4$ systems), and attributed the decrease in $[U]_{aq}$ to a reduction to U(IV) and a solubility control by UO_2(am, hyd). In hyperalkaline pH conditions, the authors obtained significantly higher uranium concentrations after an equilibration time of 56 days (see Fig. 4b.). The increased solubility combined with the observed pH-dependency was explained by Fujiwara and co-workers by the formation of $U^{IV}(OH)_5^-$ and $U^{IV}(OH)_6^{2-}$ species in equilibrium with UO_2(am, hyd). We note that very different $[U(VI)]_0$ were used in Fujiwara et al. (2005) ($1{\cdot}10^{-3}$ M) and in the present work ($3.0{\cdot}10^{-5}$ M). As discussed in Section 4.1.2, reduction kinetics are strongly affected by $[U(VI)]_0$, and this can expectedly be the reason for the different behaviour observed among the available studies. Such disagreement is discussed in detail in Section 4.3. Ryan and Rai (1983) performed solubility experiments with UO_2(am, hyd) precipitated in alkaline conditions from an acidic U(IV) stock solution. The authors used $Na_2S_2O_4$ as holding reducing agent in their experiments. Most of the solubility data reported by Ryan and co-workers in hyperalkaline conditions scatter around ≈10^{-8} M (see Fig. 4b.), clearly below the solubility data reported in Fujiwara et al. (2005) and in good agreement with our final U concentrations. The increase in solubility observed by Ryan and co-workers at $pH_m \approx 14$ was explained by the authors with the oxidation to U(VI).

4.1.3. Sn(II) + TiO_2 systems in 0.1 M NaCl

Fig. 5 shows the redox behaviour of uranium in the presence of 20 mM Sn(II) + 10 mg TiO_2 in 0.1 M NaCl solutions with $2 \leq pH_m \leq 12.8$. Experimental E_h values summarized in Fig. 5a are in line with E_h values measured in pure Sn(II) systems, and are in all cases situated within the stability field of U(IV). Fig. 5b shows that the initial concentration of uranium decreases rapidly (≈ 37 days) to values consistent with a complete reduction to U(IV) and a solubility control by UO_2(am, hyd). As in pure Sn(II) systems, however, a significantly slower reduction takes place at $pH_m \approx 6$.

The comparison of Fig. 5b with Figs. 1b and 2b shows that under analogous (pe + pH_m) conditions, the presence of TiO_2 accelerates the reduction of U(VI) to U(IV).[4] This is consistent with the known role of TiO_2 in catalysing redox processes (Wehrli et al., 1989; Amadelli et al., 1991; Tan et al., 2003). Enhanced kinetics are promoted by the strong sorption of U(VI) (and An(VI) in general) on TiO_2 over a broad range of

[4] No special precaution was taken to avoid the light exposure to those samples prepared in the presence of TiO_2.

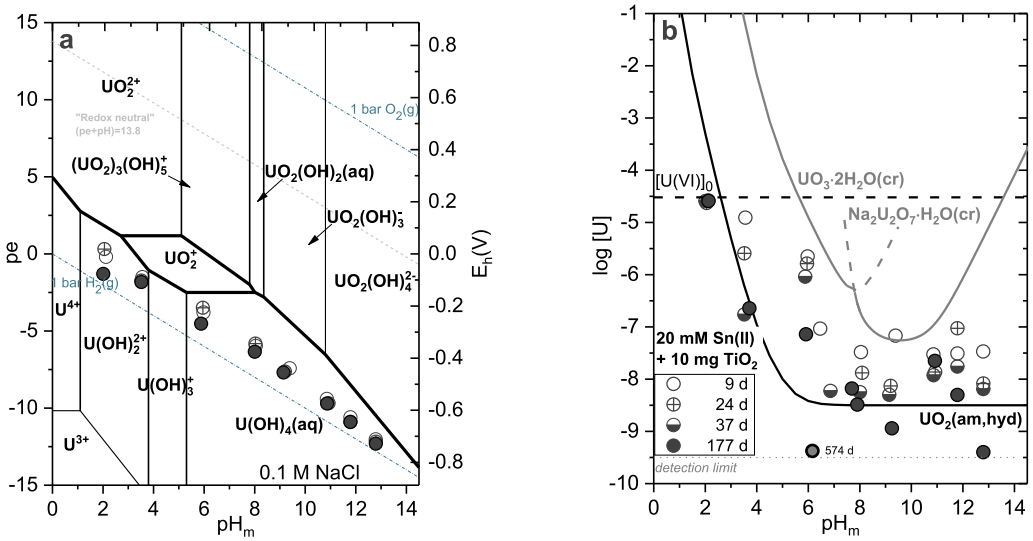

Fig. 5. a. Pourbaix diagram of uranium calculated for [U] = $3.0{\cdot}10^{-5}$ M and 0.1 M NaCl. Calculations performed allowing the precipitation of $UO_3{\cdot}2H_2O$(cr), $Na_2U_2O_7{\cdot}H_2O$(cr) and UO_2(am, hyd). Symbols represent experimentally measured E_h and pH_m values in 0.1 M NaCl systems containing 20 mM Sn(II) + 10 mg TiO_2; b. concentrations of uranium measured after 10 kD ultrafiltration for 0.1 M NaCl systems with [Sn(II)] = 20 mM + 10 mg TiO_2 and $[U(VI)]_0 = 3.0{\cdot}10^{-5}$ M. Solid lines correspond to solubility curves of $UO_3{\cdot}2H_2O$(cr), $Na_2U_2O_7{\cdot}H_2O$(cr) and UO_2(am, hyd) calculated using thermodynamic data in Section 2. Dashed horizontal line indicates the initial U(VI) concentration in the experiments. The different filling of the data points refers to the different equilibration times.

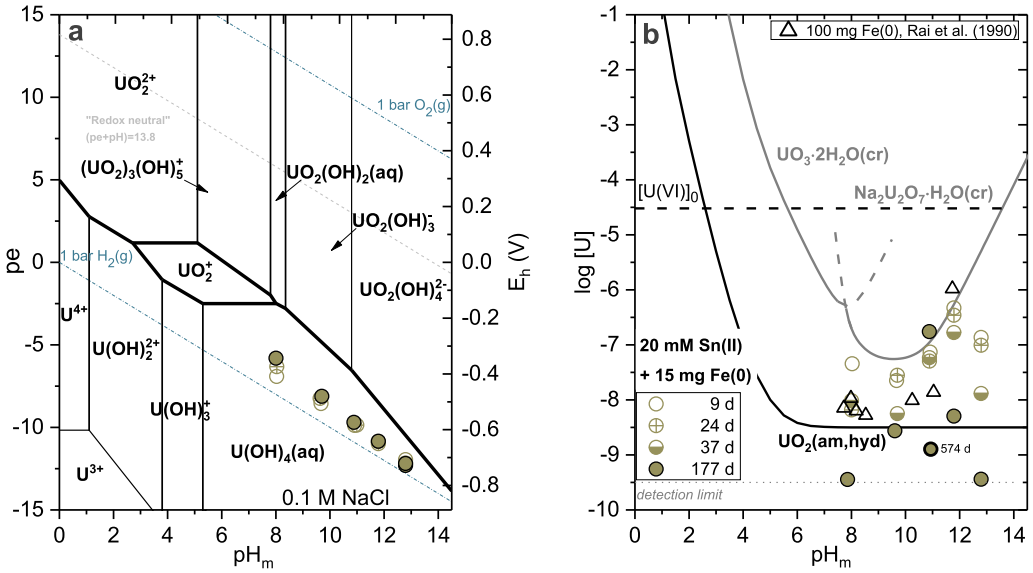

Fig. 6. a. Pourbaix diagram of uranium calculated for [U] = $3.0{\cdot}10^{-5}$ M and 0.1 M NaCl. Calculations performed allowing the precipitation of $UO_3{\cdot}2H_2O$(cr), $Na_2U_2O_7{\cdot}H_2O$(cr) and UO_2(am, hyd). Symbols represent experimentally measured E_h and pH_m values in 0.1 M NaCl systems containing 20 mM Sn(II) + 15 mg Fe(0); b. concentrations of uranium measured after 10 kD ultrafiltration for 0.1 M NaCl systems with [Sn(II)] = 20 mM + 15 mg Fe(0) and $[U(VI)]_0 = 3.0{\cdot}10^{-5}$ M; black triangle: solubility of UO_2(am, hyd) in Fe(0) systems as reported in Rai et al. (1990). Solid lines correspond to solubility curves of $UO_3{\cdot}2H_2O$(cr), $Na_2U_2O_7{\cdot}H_2O$(cr) and UO_2(am, hyd) calculated using thermodynamic data in Section 2. Dashed horizontal line indicates the initial U(VI) concentration in the experiments. The different filling of the data points refers to the different equilibration times.

pH (Eliet and Bidoglio, 1998; Den Auwer et al., 2003; Lefevre et al., 2008; Schmidt and Vogelsberger, 2009; Comarmond et al., 2011; Tits et al., 2014).

4.1.4. Sn(II) + Fe(0) and Sn(II) + Fe_3O_4(cr) systems in 0.1 M NaCl

Figs. 6a and 7a show the experimental E_h and pH_m values measured in systems containing 20 mM Sn(II) + 15 mg Fe(0) and 20 mM Sn(II) + 10 mg Fe_3O_4(cr), respectively. Both datasets are plotted in *Pourbaix* diagrams of uranium calculated for 0.1 M NaCl solutions with [U] = $3.0{\cdot}10^{-5}$ M using thermodynamic data summarized in Section 2. Very similar and low E_h values (pe + pH_m = 2 ± 1) are measured in both systems. These values are in excellent agreement with E_h values measured in Sn(II) systems but in absence of Fe phases (see Section 4.1.1), thus indicating that redox potential is governed by Sn(II) rather than by Fe.

Figs. 6b and 7b show the concentrations of U measured in Sn(II) + Fe(0) and Sn(II) + Fe_3O_4(cr) systems, respectively. For both systems and in samples at $pH_m \leq 10$, the initial concentration of U decreases very rapidly ($t \approx 37$ days) to very low values ($< 10^{-8}$ M), consistently with the reduction of U(VI) to U(IV) and a solubility-control by UO_2(am, hyd). Slower reduction kinetics are observed at $pH_m \geq 11$ in both Fe systems (up to 574 days are required at $pH_m \approx 11$). Similar observations were recently reported by Bruno et al. (2018), who investigated the redox behaviour of uranium under

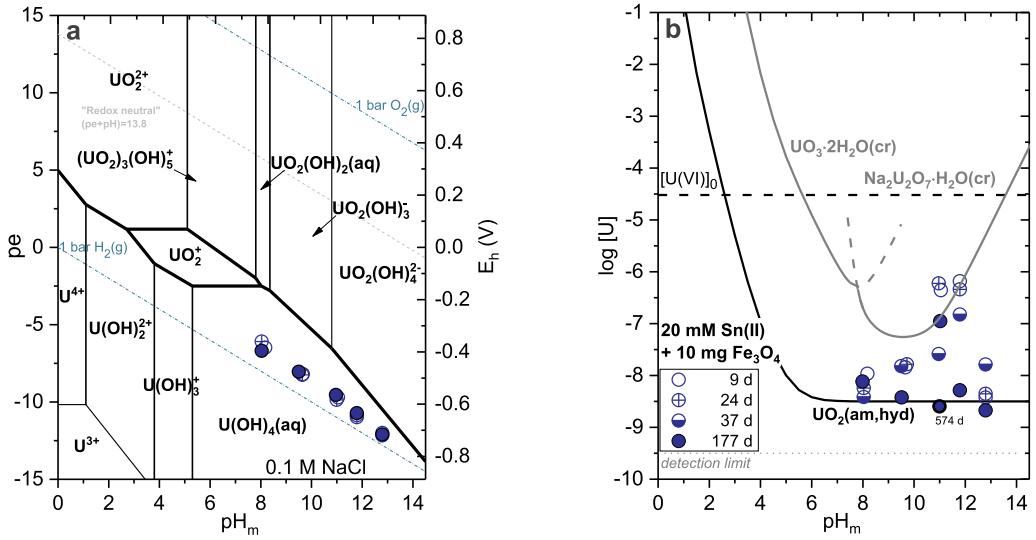

Fig. 7. a. Pourbaix diagram of uranium calculated for [U] = $3.0{\cdot}10^{-5}$ M and 0.1 M NaCl. Calculations performed allowing the precipitation of $UO_3{\cdot}2H_2O$(cr), $Na_2U_2O_7{\cdot}H_2O$(cr) and UO_2(am, hyd). Symbols represent experimentally measured E_h and pH_m values in 0.1 M NaCl systems containing 20 mM Sn(II) + 10 mg Fe_3O_4(cr); b. concentrations of uranium measured after 10 kD ultrafiltration for 0.1 M NaCl systems with [Sn(II)] = 20 mM + 10 mg Fe_3O_4(cr) and $[U(VI)]_0$ = $3.0{\cdot}10^{-5}$ M. Solid lines correspond to solubility curves of $UO_3{\cdot}2H_2O$(cr), $Na_2U_2O_7{\cdot}H_2O$(cr) and UO_2(am, hyd) calculated using thermodynamic data in Section 2. Dashed horizontal line indicates the initial U(VI) concentration in the experiments. The different filling of the data points refers to the different equilibration times.

alkaline reducing conditions. For a system at pH_m = 12.8 in the presence of Sn(II) + Fe_3O_4(cr), the authors reported the slow decrease of the original uranium concentration, and confirmed by XPS analysis that U(IV) was predominant in the solid phase. Rai et al. (1990) studied the solubility of U(IV) with UO_2(am, hyd) precipitated in alkaline conditions from an acidic U(IV) stock solution. The authors used Fe(0) as holding reducing agent to retain uranium in the +IV redox state. We note that very short equilibration times ($t \leq 6$ days) were considered in this solubility study. The solubility data reported by Rai et al. at $pH \leq 11$ is in good agreement with our long-term redox experiments in the presence of Sn(II) + Fe(0) (see Fig. 6b.). The authors attributed the increased uranium concentration at pH ≈ 12 to the likely oxidation of U(IV) to U(VI). We agree with this hypothesis, and provide a further insight on this discussion: although Fe(0) sets very reducing conditions (close to the border of water reduction) within a broad range of alkaline conditions ($pH_m < 11$), it has been shown that the passivation / corrosion of the surface of Fe(0) occurring in hyperalkaline pH_m conditions results in a significant increase of the redox potential (Kobayashi et al., 2013; Bruno et al., 2018; Yalcintas et al., 2015). Bruno and co-workers showed that the (pe + pH_m) conditions set by Fe(0) at pH_m = 12.8 were above the redox borderline of U(VI) / U(IV), and confirmed that no reduction of U(VI) to U(IV) was observed in this system. Unfortunately, Rai et al. did not report E_h values in his paper and our hypothesis (though plausible) cannot be confirmed. The discussion above highlights that in our redox experiments with Sn(II) + Fe(0) and Sn(II) + Fe_3O_4(cr), Sn(II) is indeed the system controlling the redox behaviour of uranium.

4.2. Redox speciation of uranium in the aqueous and solid phases

4.2.1. Solvent extraction

The solvent extraction method described in Section 3.3. was used to assess the redox state of uranium in samples with [U] ≥ 10^{-5} M. Because of the low solubility of U(IV) at $pH_m \geq 4$, the extraction method was restricted to samples with $2 \leq pH_m \leq 3.1$. The results obtained for selected acidic samples are summarized in Table 4. In all cases, solvent extraction confirms the predominance of U(IV) in solution (≥97%) after attaining equilibrium conditions. This observation is in agreement with thermodynamic calculations provided in Figs. 2a – 5a.

4.2.2. XANES analysis

Fig. 8 shows the U L_{III}-edge XANES spectra of selected aqueous (Fig. a., ACT-Beamline) and solid (Fig. b., INE-Beamline) samples, including reference spectra of aqueous species / solid compounds of U(VI) and U(IV) collected at the same beamlines. The experimental conditions and edge positions (white line, WL) are summarized in Table 5. We note that significant differences arise in the WL of U(VI) and U(IV) references for aqueous and solid samples. The use of different beamlines can be partly responsible for such differences. However, intrinsic differences between aqueous and solid moieties are known to importantly impact edge positions for a given actinide and redox state (see for instance discussion on XAFS of Np(V) and Np(VI) aqueous species and solid compounds in alkaline systems Gaona et al., 2012). For these reasons, the use of similar reference systems measured at the same beamline is mandatory for the correct assessment of the redox state of a given (actinide) system.

The edge position of the aqueous sample containing 20 mM Sn(II) in 0.1 M NaCl at $pH_m \approx 2$ is in excellent agreement with the position of the U(IV) reference (see Fig. 8a and Table 5), thus confirming that uranium is found in the +IV redox state. This is in line with thermodynamic calculations and with results obtained for the same sample by solvent extraction.

Fig. 8b shows the XANES spectra of solid uranium samples collected

Table 4
Fraction of U(IV) in the aqueous phase of selected solubility samples in acidic, dilute to concentrated NaCl solutions, as quantified by solvent extraction after 10 kD ultrafiltration.

Sample	pH_m[a]	E_h [mV][b]	U(IV) [%][c]
0.1 M NaCl, 20 mM Sn(II)	2.2	−284	98%
0.1 M NaCl, 20 mM Sn(II) + 10 mg TiO_2	2.1	−357	97%
5.0 M NaCl, 20 mM Sn(II)	3.1	−288	99%

a: ± 0.05; b: ± 20 mV; c: ± 10%.

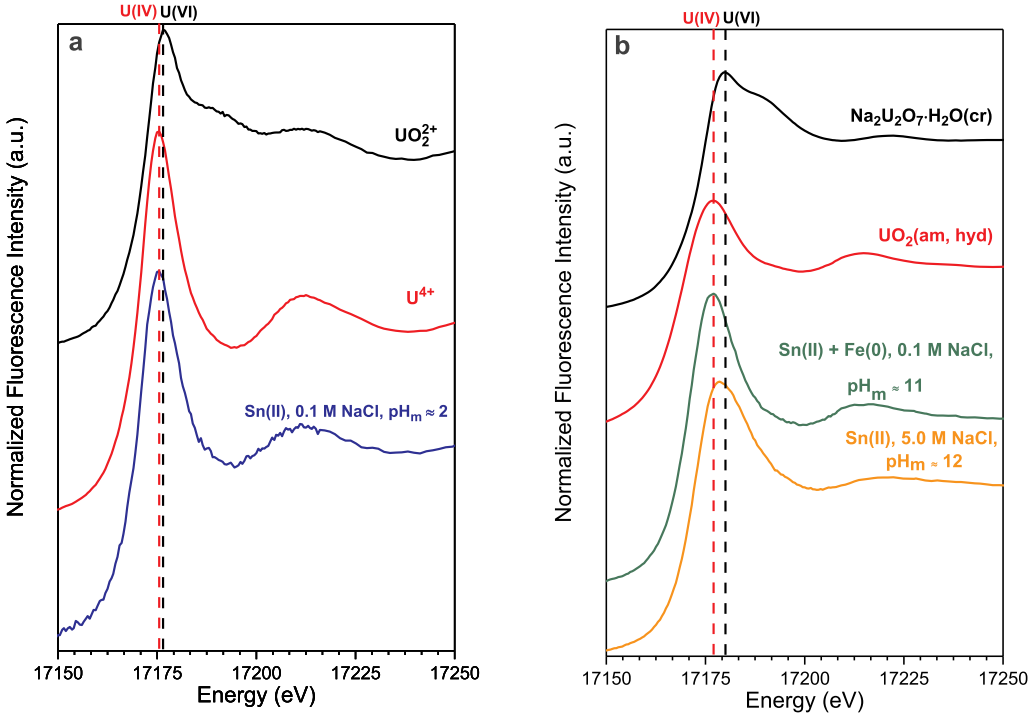

Fig. 8. U L_{III} XANES spectra collected for (a) aqueous sample in 0.1 M NaCl, 20 mM Sn(II) at $pH_m \approx 2$; (b) uranium solid phases collected from solubility experiments in 0.1 M NaCl, 20 mM Sn(II) + 15 mg Fe(0) at $pH_m \approx 11$ (green line), and in 5.0 M NaCl, 20 mM Sn(II) at $pH_m \approx 12$. Black and red spectra in (a) and (b) correspond to U(VI) and U(IV) references, respectively. (For interpretation of the references to colour in this figure legend, the reader is referred to the Web version of this article.)

Table 5
XANES results of aqueous and solid phases in selected solubility samples. U(VI) and U(IV) references measured at ACT- and INE-Beamline for aqueous species and solid compounds, respectively.

Sample	pH_m[a]	E_h[b]	Contact time [days]	Edge position (eV)	Beamline
Aqueous phase					
Reference U(VI), 1.0 M HCl	≈0	n. m.		17176.5	ACT
Reference U(IV), 1.0 M HCl, 20 mM Sn(II)	≈0	n. m.		17175.2	ACT
0.1 M NaCl, 20 mM Sn(II)	2.2	−284	330	17175.2	ACT
Solid phase					
Reference $Na_2U_2O_7{\cdot}H_2O$(cr)	≈12	n. m.		17180.0	INE
Reference UO_2(am, hyd)	≈12	n. m.		17177.0	INE
0.1 M NaCl, 20 mM Sn(II) + Fe(0)	10.9	−798	330	17177.0	INE
5.0 M NaCl, 20 mM Sn(II)	11.9	−799	330	17178.5	INE

a: ± 0.05; b: ± 20 mV.

from solubility experiments in (i) 0.1 M NaCl at pH_m = 10.9, with 20 mM Sn(II) + 15 mg Fe(0), and (ii) 5.0 M NaCl at pH_m = 11.9, with 20 mM Sn(II). The edge position of the solid sample in 0.1 M NaCl is in excellent agreement with the edge position of UO_2(am, hyd) reference. A significant shift to higher energies (≈ +1.5 eV, compared to the edge position of UO_2(am, hyd)) is observed for the uranium solid equilibrated in 5.0 M NaCl. The XANES spectra of this sample does not show, however, the typical shoulder of the uranyl or uranate (in $Na_2U_2O_7{\cdot}H_2O$(cr)) moieties. These observations suggest the predominance of U(IV) in the solid phase, albeit with a significant contribution of U(VI).

The process of reduction of the initial aqueous U(VI) in alkaline NaCl solutions goes through a first, fast precipitation of $Na_2U_2O_7{\cdot}H_2O$(cr) followed by a slow transformation of this solid phase into UO_2(am, hyd). As discussed in Section 4.1, the kinetics of this transformation are affected by $[U(VI)]_0$, [Sn(II)] and pH_m. Beyond these parameters, the concentration of sodium in solution participates in the equilibrium reaction driving the transformation of $Na_2U_2O_7{\cdot}H_2O$(cr) into UO_2(am, hyd):

$$0.5\,Na_2U_2O_7{\cdot}H_2O(cr) + 2\,e^- + 3\,H^+ \leftrightarrow UO_2(am, hyd) + Na^+ + 2\,H_2O(l) \quad (6)$$

with

$$\log {}^*K^\circ_{s,0}\{0.5\,Na_2U_2O_7{\cdot}H_2O(cr)\} = \log {}^*K^\circ_{s,0}\{UO_2(am, hyd)\} + \log [Na^+] + \log \gamma_{Na^+} + 3\,pH_m - 3\log \gamma_{H^+} + 2\,pe + 2\log a_w \quad (7)$$

The combination of solubility data and XANES indicates that a contact time of 330 days was sufficient to transform completely $Na_2U_2O_7{\cdot}H_2O$(cr) into UO_2(am, hyd) in a 0.1 M NaCl solution with $pH_m \approx 11$, but insufficient to complete such transformation in a 5.0 M

NaCl solution with $pH_m \approx 12$. This is in line with reaction (6) and corresponding equation (7), which indicate that such transformation is favoured at low pH_m, pe and $[Na^+]$.

4.3. Kinetic aspects of U(VI) reduction to U(IV): main results in the present study and comparison with literature data

Multielectron transfer processes involving changes in the structure of the redox counterparts are known to be kinetically hindered (Morel and Hering, 1996; Stumm and Morgan, 1996; Altmaier et al., 2011). Such impact on kinetics is also known in the case of light actinides U, Np, Pu and Am, which form two structurally different moieties (An^{x+} and AnO_2^{y+}) for the lower (+3 and + 4, x = 3–4) and higher (+5 and + 6, y = 1–2) oxidation states (Sullivan et al., 1957; Lemire et al., 2001; Hennig et al., 2009, 2010). The kinetics of U(VI) reduction have been largely investigated in the literature, with special focus on systems containing Fe and often looking at the impact of surfaces on the reduction process (Liger et al., 1999b; Rovira et al., 2007; Duro et al., 2008; Yan et al., 2014). However, most of these efforts have been dedicated to the study of the near-neutral pH-range, leaving aside alkaline to hyperalkaline pH conditions as those defined by cementitious systems. This is possibly due to the experimental challenges related to these boundary conditions which require a strict exclusion of O_2 and CO_2. Such experimental challenges are likely the reason for the discrepancies in the literature on the solution chemistry of U(IV) and the corresponding implications in the U(VI) / U(IV) redox boundaries.

Experimental results presented in Sections 4.1.1 to 4.1.4 demonstrate our success in retaining very reducing conditions for equilibration times up to 635 days. In these conditions, thermodynamic data summarized in Section 2 predict the predominance of U(IV) aqueous species and solid compounds within the complete pH_m-range investigated in the present study ($2 \le pH_m \le 14.5$, see Figs. 1 to 7.). The discussion in Sections 4.1.1 to 4.1.4 already hint to a remarkable impact of kinetics on the reduction process, with $[U(VI)]_0$, $[Sn(II)]$, pH_m, pe and $[Na^+]$ identified as main parameters affecting kinetics of U(VI) reduction in the conditions of our study. This section provides an accurate rapport of the time-dependency observed for the systems investigated in the present work. Focus is given to hyperalkaline pH_m conditions ($10 \le pH_m \le 13.5$), and comparison with literature data is provided whenever available.

Fig. 9 Evaluates the impact of $[U(VI)]_0$ and concentration of the reducing chemical on the reduction kinetics of U(VI) at $pH_m \approx 13$. The figure includes also thermodynamic calculations for the solubility of U(VI) (as $Na_2U_2O_7{\cdot}H_2O$(cr)) and U(IV) (as UO_2(am, hyd)) using thermodynamic data summarized in Section 2. A third calculated solubility is appended to the figure using thermodynamic data reported in Fujiwara et al. (2005) for the anionic hydrolysis species of U(IV), $U(OH)_5^-$ and $U(OH)_6^{2-}$.

Fig. 9a shows that for the system at $pH_m \approx 13$ with lowest $[U(VI)]_0$ ($3{\cdot}10^{-5}$ M) and highest [Sn(II)] (20 mM), U(VI) is completely reduced to U(IV) after ≈ 50 days. A much longer contact time (≈ 600 days) is required to reach a complete reduction for the system with highest $[U(VI)]_0$ ($4{\cdot}10^{-4}$ M) and lowest [Sn(II)] (2 mM). In the latter case and up to $t \approx 250$ days, the concentration of uranium in solution is consistent with the solubility of UO_2(am, hyd) calculated including the formation of $U(OH)_5^-$ and $U(OH)_6^{2-}$ as reported in Fujiwara et al. (2005). However, we note that this uranium concentration is also consistent with a solubility-control by the reaction $0.5\ Na_2U_2O_7{\cdot}H_2O(cr) + 2\ H_2O(l) \leftrightarrow UO_2(OH)_4^{2-} + Na^+ + H^+$ with $\log {}^*K_{s,(1,4)} = -(19.05 \pm 0.1)$ (calculated from Altmaier et al., 2017). As discussed in the previous section, the concentration of uranium in the reduction of U(VI) from oversaturation conditions is governed by two processes: a first, fast decrease in concentration controlled by the precipitation of U(VI) solid phases, followed by a slow transformation of this solid phase into UO_2(am, hyd). In the system under discussion ($[U(VI)]_0 = 4{\cdot}10^{-4}$ M and [Sn(II)] = 2 mM), UO_2(am, hyd) certainly forms from the beginning of the experiment, but the most soluble solid phase present in the system ($Na_2U_2O_7{\cdot}H_2O$(cr)) controls $[U]_{aq}$ for contact times up to $t \approx 250$ days. Only after this very long contact time, $[U]_{aq}$ decreases further until reaching the level corresponding to a solubility-control by UO_2(am, hyd) at $t \approx 600$ days.

Fig. 9b shows the reduction kinetics of U(VI) as determined at $pH_m \approx 13$ for systems containing $Na_2S_2O_4$ as reducing chemical

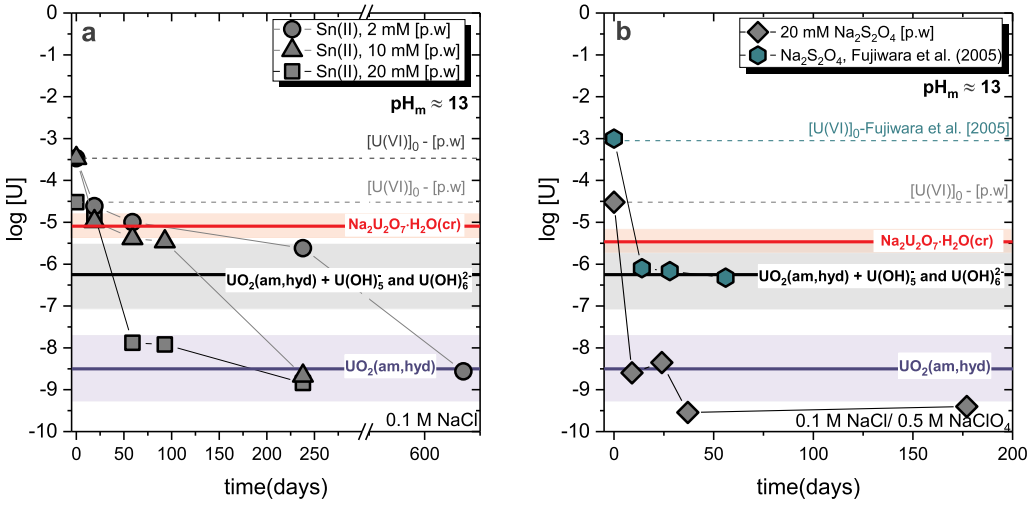

Fig. 9. Evolution of log [U] with time in reducing systems at $pH_m \approx 13$: **a**. Sn(II) systems with $[U(VI)]_0 = 4.2{\cdot}10^{-4} - 3{\cdot}10^{-5}$ M and [Sn(II)] = 2–20 mM, as determined in the present work; **b**. $Na_2S_2O_4$ systems as determined in the present work and reported by Fujiwara et al. (2005) (in 0.5 M $NaClO_4$–NaOH). Solid horizontal lines in the figures correspond to the solubility of $Na_2U_2O_7{\cdot}H_2O$(cr) (red, Fig. 9a for 0.1 M NaCl–NaOH and Fig. 9b for 0.5 M NaCl–NaOH) and UO_2(am, hyd) (blue) calculated at $pH_m = 13$ using thermodynamic data summarized in Section 2. Black line corresponds to the solubility of UO_2(am, hyd) calculated including the formation of $U(OH)_5^-$ and $U(OH)_6^{2-}$ as reported in Fujiwara et al. (2005). Coloured area (in red / grey / blue) gives an indication of the uncertainty in the given solubility equilibria. Dashed horizontal lines indicate the initial U(VI) concentration in the experiments. (For interpretation of the references to colour in this figure legend, the reader is referred to the Web version of this article.)

(present work and Fujiwara et al., 2005). A very fast decrease of $[U]_{aq}$ to $\approx 10^{-8.5}$ M is observed in our study after $t = 9$ days, consistently with a complete reduction to U(IV) and in excellent agreement with a solubility control by UO_2(am, hyd). In contrast to this observation, Fujiwara and co-workers reported a significantly higher uranium concentration ($\approx 10^{-6}$ M) after $t \approx 50$ days, when these authors interrupted the experiment. These results were the basis for the proposed formation of $U(OH)_5^-$ and $U(OH)_6^{2-}$ species, in equilibrium with UO_2(am, hyd). Although not shown in Fig. 9b., the solubility data reported by Ryan and Rai (1983) with UO_2(am, hyd) precipitated from a U(IV) stock solution and using $Na_2S_2O_4$ as holding reducing agent lead to $[U]_{aq}$ in excellent agreement with our observations.

Key differences arise in the experimental approach by Fujiwara et al. and in our work that can help to understand the apparent contradictions between both studies. Hence, a significantly higher $[U(VI)]_0$ was used in Fujiwara et al. (2005) compared to the present work ($1{\cdot}10^{-3}$ M *vs.* $3{\cdot}10^{-5}$ M). As discussed in section 4.1.1 and also shown in Fig. 9a., $[U(VI)]_0$ has a relevant impact on the reduction kinetics, and up to 600 days were required to completely reduce to U(IV) an initial U(VI) concentration of $4{\cdot}10^{-4}$ M. Both experimental studies also differ in the concentration of Na used as background electrolyte (0.5 M $NaClO_4$ in Fujiwara et al. *vs.* 0.1 M NaCl in the present work[5]). As discussed in Section 4.2.2, the driving force for the transformation of $Na_2U_2O_7{\cdot}H_2O$(cr) into UO_2(am, hyd) decreases with increasing concentration of Na (see equilibrium reaction (6)). Based on these observations, we firmly believe that the interpretation in Fujiwara et al. (2005) is flawed by insufficient equilibration time. Solubility data reported after $t \approx 50$ days is likely controlled by the equilibrium $0.5\,Na_2U_2O_7{\cdot}H_2O(cr) + (x{-}2)\,H_2O(l) \leftrightarrow UO_2(OH)_x^{2-x} + Na^+ + (x{-}3)\,H^+$, with $x = 3$–4.[6] We hypothesize that the authors would have observed a second step in the overall decrease of $[U]_{aq}$ at longer equilibration times corresponding to a solubility control by UO_2(am, hyd). Similar conclusions can be drawn when comparing their and our observations at $pH_m = 12$ (data not shown).

Fig. 10 shows the reduction kinetics of U(VI) at $pH_m = 8-13$ in the presence of different reducing systems (Sn(II), Sn(II) + Fe(0), Sn(II) + Fe_3O_4(cr) and Sn(II) + TiO_2). We note that concentration of Sn(II) was the same in all these systems (20 mM), and thus this exercise aimed at evaluating the impact of different surfaces on the overall reduction kinetics. Fig. 10 includes also thermodynamic calculations for the solubility of U(VI) (as $Na_2U_2O_7{\cdot}H_2O$(cr)) and U(IV) (as UO_2(am, hyd)) solid phases using thermodynamic data summarized in Section 2.

Fig. 10 shows a relatively fast reduction in all systems investigated in the presence of 20 mM Sn(II). The interpretation of such diagrams requires a clear understanding of some key parameters:

- TiO_2, Fe_3O_4(cr) and Fe(0) provide surfaces that can expectedly catalyse the reduction of U(VI) to U(IV). However, Sn(II) precipitates also as sparingly soluble SnO(s) (or analogous oxo-hydroxides). Sn(II) surfaces can possibly participate in the catalysis of U(VI) reduction.
- Sn(II) shows an amphoteric behaviour, forming cationic and anionic hydrolysis species in acidic and alkaline pH conditions, respectively). Consequently, all Sn(II) systems except those at $pH_m \approx 13$ include solid SnO(s) (approximately 50 mg). At this pH_m, the enhancement in the solubility due to the formation of $Sn(OH)_3^-$ leads to the complete dissolution of SnO(s) (see Fig. S1 in Supporting Information).
- The solubility of $Na_2U_2O_7{\cdot}H_2O$(cr) is about 2 orders of magnitude lower at $pH_m = 8-11$ than at $pH_m \approx 13$, whereas the solubility of UO_2(am, hyd) remains the same within $8 \leq pH_m \leq 13$. This leads to a greater difference in the solubility of U(VI) and U(IV) under hyperalkaline conditions, compared to weakly alkaline pH_m.

No significant differences can be identified in the reduction kinetics of U(VI) at $pH_m = 8-11$ for the systems Sn(II), Sn(II) + TiO_2, Sn(II) + Fe(0) and Sn(II) + Fe_3O_4(cr). As discussed in Section 4.1.3 slightly faster reduction kinetics can be claimed in the presence of TiO_2 at $pH_m \geq 12$.

Most of the systems described in Fig. 10a – c. show a first step in the decrease of $[U(VI)]_0$ where uranium concentration stabilizes at 10^{-7} – 10^{-8} M, followed by a final step where uranium concentration decreases clearly below $\approx 10^{-8}$ – $10^{-9.5}$ M. Although less evident than the process described above for samples at $pH_m \approx 13$, this observation might be attributed again to a first, fast decrease in concentration controlled by the precipitation of $Na_2U_2O_7{\cdot}H_2O$(cr), followed by a slow transformation of this U(VI) solid phase into UO_2(am, hyd).

5. Conclusions

The redox behaviour of uranium was investigated in reducing, dilute to concentrated NaCl solutions covering a broad pH_m-range (2 – 14.5). Special focus was put on alkaline to hyperalkaline systems due to the ill-defined U(VI) / U(IV) redox borderline under these conditions and the controversy on the existence of anionic species of U(IV). Uranium was added to independent batch samples as U(VI), and the evolution of uranium concentration in five different reducing systems (Sn(II), $Na_2S_2O_4$, Sn(II) + Fe(0), Sn(II) + TiO_2 and Sn(II) + Fe_3O_4) monitored for $t \leq 635$ days.

After attaining equilibrium conditions, the measured low uranium concentrations in solution was in most cases in good agreement with the solubility of UO_2(am, hyd), strongly supporting the reduction of U(VI) to U(IV). This observation is in line with results obtained by solvent extraction and XANES, which confirm that uranium is predominantly found as U(IV) in the aqueous and solid phases investigated. Kinetics play a very important role in the reduction process, and are importantly affected by $[U(VI)]_0$, pH_m, E_h, concentration of the reducing chemical and presence of redox-active surfaces. Our results provide also insight in the mechanism driving the reduction of U(VI) in alkaline NaCl systems: a first, fast precipitation of $Na_2U_2O_7{\cdot}H_2O$(cr) is followed by the slow transformation of this U(VI) solid phase into UO_2(am, hyd). Such transformation is favoured at low pH_m, pe and Na concentrations. Our results strongly support the predominance of the species $U(OH)_4$(aq) (or analogous, neutral polyatomic species) up to pH_m values of 14.5, thus disregarding the formation of U(IV) anionic hydrolysis species ($U(OH)_5^-$ and $U(OH)_6^{2-}$) as proposed in previous studies. As discussed by Ryan and Rai (1983), oxidation of U(IV) is suspected to have occurred in Gayer and Leider (1957) and Tremaine et al. (1981). We suggest that also the study by Fujiwara et al. (2005) is possibly flawed by insufficient equilibration time, which prevented the complete reduction of the initial U(VI) to U(IV).

Experimental observations in the present work (pH_m, E_h, solubility) are in excellent agreement with thermodynamic calculations (Pourbaix diagrams, solubility curves) using the NEA–TDB thermodynamic selection, complemented with data reported in Neck and Kim (2001) and Altmaier et al. (2017) for U(IV) and U(VI) species, respectively. This suggests that experimental pH_m and E_h values measured in buffered

[5] These concentrations correspond to the examples shown in Fig. 9b. Fujiwara and co-workers performed also experiments in 1.0 and 2.0 M $NaClO_4$–NaOH with similar results. Experiments performed in the present work in 5.0 M NaCl–NaOH solutions (in 20 mM Sn(II) and with $[U(VI)]_0 = 3{\cdot}10^{-5}$ M) showed: (i) a good agreement with the solubility of $Na_2U_2O_7{\cdot}H_2O$(cr) at $pH_m \approx 13$ after an equilibration of 65 days (thus incomplete reduction to U(IV), see solubility data in Fig. 3b), and (ii) an incomplete transformation of $Na_2U_2O_7{\cdot}H_2O$(cr) into UO_2(am, hyd) at $pH_m \approx 12$ after 330 days (see XANES results in Section 4.2.2).

[6] The authors claim the identification of UO_2(am, hyd) by XRD, but do not show the corresponding diffractogram in the publication. As reported in Altmaier et al. (2017), $Na_2U_2O_7{\cdot}H_2O$(cr) shows rather broad and less intense XRD reflections, which could have been easily missed by Fujiwara and co-workers in the evaluation of their XRD data.

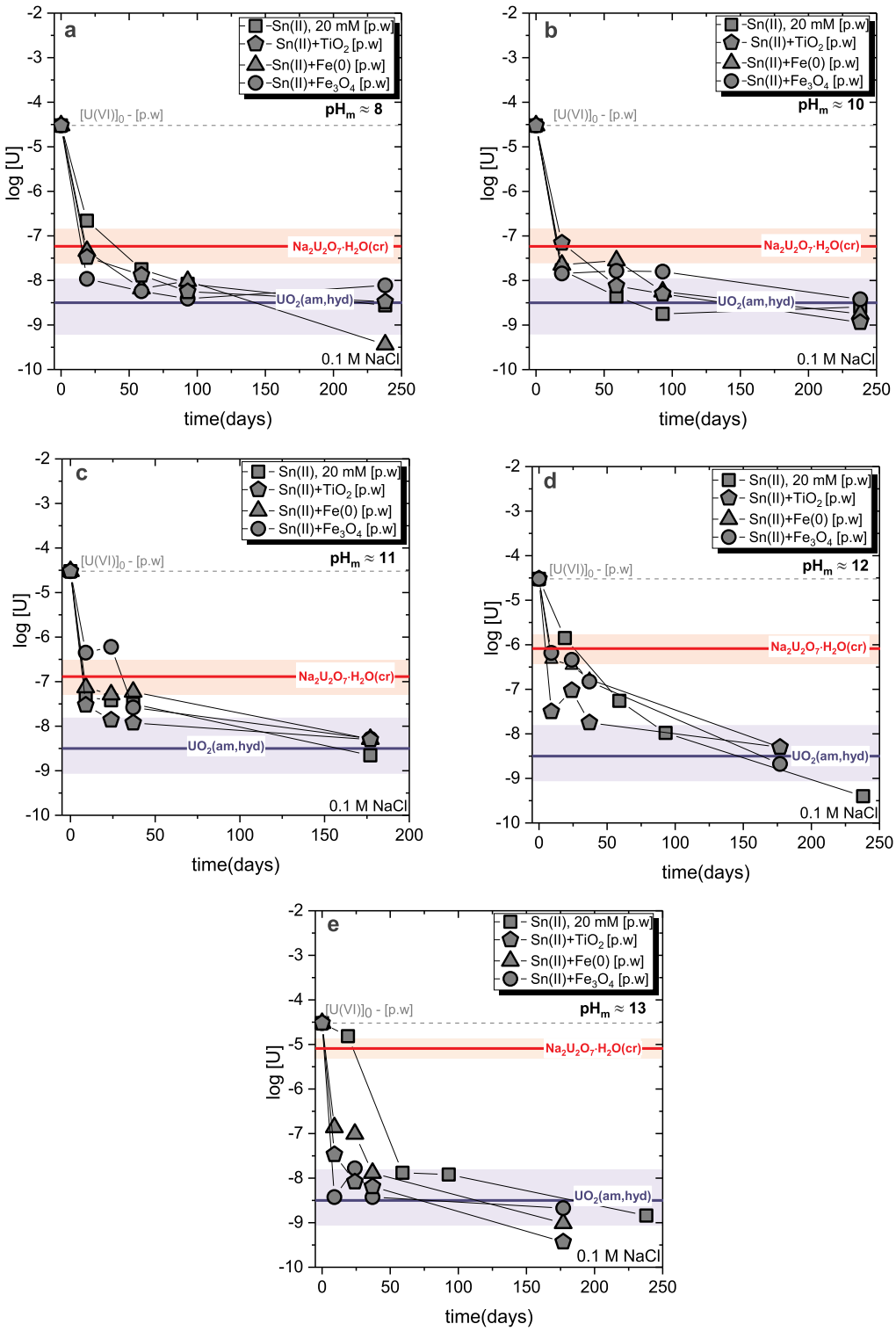

Fig. 10. Evolution of log [U] with time in reducing systems with presence of Sn(II), Sn(II) + TiO_2, Sn(II) + Fe(0) and Sn(II) + Fe_3O_4(cr) at: a. $pH_m \approx 8$, compared with the data reported by Cantrell et al. (1995); b. $pH_m \approx 10$; c. $pH_m \approx 11$ and d. $pH_m \approx 12$ and e. $pH_m \approx 13$. Solid horizontal lines in the figures correspond to the solubility of $Na_2U_2O_7{\cdot}H_2O$(cr) (red) and UO_2(am, hyd) (blue) calculated at the corresponding pH_m using thermodynamic data summarized in Section 2. Coloured area (in red / blue) gives an indication of the uncertainty in the given solubility equilibria. Dashed horizontal line indicate the initial U(VI) concentration in the experiments. (For interpretation of the references to colour in this figure legend, the reader is referred to the Web version of this article.)

systems in combination with available thermodynamic data can be reliably used for the prediction of the redox state distribution of uranium in dilute to concentrated NaCl systems under boundary conditions relevant for nuclear waste disposal.

Acknowledgements

The authors would like to thank colleagues at KIT–INE who have contributed to this work: David Fellhauer and Vanessa Montoya for fruitful discussions and comments; Ivan Pidchenko and Yuri Totskiy for

the synthesis of magnetite; Melanie Böttle, Frank Geyer and Cornelia Walschburger for their technical support. We acknowledge the KIT light source for provision of instruments at the INE-Beamline/ACT experimental station operated by the Institute of Nuclear Waste Disposal and we would like to thank the Institute for Beam Physics and Technology (IBPT) for the operation of the storage ring, the Karlsruhe Research Accelerator (KARA). This study was funded by the German Ministry of Economic Affairs and Energy (BMWi) within the framework of the EDUKEM project with contract number 02E11334.

References

Altmaier, M., Gaona, X., D, F., Buckau, G., 2011. Intercomparison of Redox Determination Methods on Designed and Near Neutral Aquesous Systems, KIT SR 7572. Karlsruhe Institute of Tehcnology Karlsruhe, 34.

Altmaier, M., Metz, V., Neck, V., Müller, R., Fänghanel, T., 2003. Solid-liquid equilibria of $Mg(OH)_2$(cr) and $Mg_2(OH)_2Cl.4H_2O$(cr) in the system Mg-Na-H-OH-O-Cl-H_2O at 25 °C. Geochem. Cosmochim. Acta 67, 3595–3601.

Altmaier, M., Yalcintas, E., Gaona, X., Neck, V., Müller, R., Schlieker, M., Fanghänel, T., 2017. Solubility of U(VI) in chloride solutions. I. The stable oxides/hydroxides in NaCl systems solubility products, hydrolysis constants and SIT coefficients. J. Chem. Thermodyn. 114, 2–13.

Amadelli, R., Maldotti, A., Sostero, S., Carassiti, V., 1991. Photodeposition of uranium oxides onto TiO_2 from aqueous uranyl solutions. J. Chem. Soc., Faraday Trans. 87, 3267–3273.

Bruno, J., Casas, I., Lagerman, B., Munoz, M., 1986. The Determination of the Solubility of Amorphous UO_2(s) and the Mononuclear Hydrolysis Constants of Uranium(IV) at 25 °C. MRS Proceedings, vol. 84.

Bruno, J., González-Siso, M.R., Duro, L., Gaona, X., Altmaier, M., 2018. Key master variables affecting the mobility of Ni, Pu, Tc and U in the near field of the SFR repository. SKB Technical Report-18–01. Swedish Nuclear Fuel and Waste Management Co, Stockholm, Sweden.

Bube, C., Metz, V., Bohnert, E., Garbev, K., Schild, D., Kienzler, B., 2013. Long–term cement corrosion in chloride–rich solutions relevant to radioactive waste disposal in rock salt – leaching experiments and thermodynamic simulations. Phys. Chem. Earth 64, 87–94.

Cantrell, K.J., Kaplan, D.I., Wietsma, T.W., 1995. Zero-valent iron for the in-situ remediation of selected metals in groundwater. J. Hazard Mater. 42, 201–212.

Casas, I., de Pablo, J., Giménez, J., Torrero, M.E., Bruno, J., Cera, E., Finch, R.J., Ewing, R.C., 1998. The role of pe, pH, and carbonate on the solubility of UO_2 and uraninite under nominally reducing conditions. Geochem. Cosmochim. Acta 62, 2223–2231.

Ciavatta, L., 1980. The specific interaction theory in equilibrium analysis. Some empirical rules for estimating iInteraction coefficients of metal ion complexes. Ann. Chim-Rome 80, 255–263.

Comarmond, M.J., Payne, T.E., Harrison, J.J., Thiruvoth, S., Wong, H.K., Aughterson, R.D., Lumpkin, G.R., Müller, K., Foerstendorf, H., 2011. Uranium sorption on various forms of titanium dioxide - influence of surface area, surface charge, and impurities. Environ. Sci. Technol. 45, 5536–5542.

Coronel, F.T., Mareva, S., Yordanov, N., 1982. Extraction of uranium(iv) from phosphoric-acid solutions with 1-phenyl-3-methyl-4-Benzoylpyrazolone-5 (PMBP). Talanta 29, 119–123.

Cui, D.Q., Spahiu, K., 2002a. On the interaction between uranyl carbonate and UO_2(s) in anaerobic solution. J. Nucl. Sci. Technol. Suppl. 3, 500–503.

Cui, D.Q., Spahiu, K., 2002b. The reduction of U(VI) on corroded iron under anoxic conditions. Radiochim. Acta 90, 623–628.

Den Auwer, C., Drot, R., Simoni, E., Conradson, S.D., Gailhanou, M., de Leon, J.M., 2003. Grazing incidence XAFS spectroscopy of uranyl sorbed onto TiO_2 rutile surfaces. New J. Chem. 27, 648–655.

Duro, L., El Aamrani, S., Rovira, M., de Pablo, J., Bruno, J., 2008. Study of the interaction between U(VI) and the anoxic corrosion products of carbon steel. Appl. Geochem. 23, 1094–1100.

El Aamrani, F.Z., Casas, I., De Pablo, J., Duro, L., Grivé, M., Bruno, J., 1999. Experimental and Modeling Study of the Interaction between Uranium(VI) and Magnetite. KB Technical Report TR-99–21. Swedish Nuclear Fuel and Waste Management Co., Stockholm, Sweden.

Eliet, V., Bidoglio, G., 1998. Kinetics of the laser-induced photoreduction of U(VI) in aqueous suspensions of TiO_2 particles. Environ. Sci. Technol. 32, 3155–3161.

Farrell, J., Bostick, W.D., Jarabek, R.J., Fiedor, J.N., 1999. Uranium removal from ground water using zero valent iron media. Ground Water 37, 618–624.

Fellhauer, D., 2013. Untersuchungen zur Redoxchemie und Löslichkeit von Neptunium und Plutonium. PhD thesis. University of Heidelberg, Germany.

Fiedor, J.N., Bostick, W.D., Jarabek, R.J., Farrell, J., 1998. Understanding the mechanism of uranium removal from groundwater by zero-valent iron using x-ray photoelectron spectroscopy. Environ. Sci. Technol. 32, 1466–1473.

Fuger, J., Grenthe, I., Neck, V., Rai, D., 2008. Chemical Thermodynamics of Thorium, Vol. 11 of Chemical Thermodynamics. Elseiver Science Publishers, Amsterdam.

Fujiwara, K., Yamana, H., Fujii, T., Kawamoto, K., Sasaki, T., Moriyama, H., 2005. Solubility of uranium(IV) hydrous oxide in high pH solution under reducing condition. Radiochim. Acta 93, 347–350.

Fujiwara, K., Yamana, H., Fujii, T., Moriyama, H., 2003. Determination of uranium(IV) hydrolysis constants and solubility product of $UO_2{\cdot}xH_2O$. Radiochim. Acta 91, 345–350.

Galkin, N.P., Stepanov, M.A., 1960. Solubility of uranium (IV) hydroxide in sodium hydroxide. Soviet J. Atom. Energy 8, 258–261.

Gaona, X., Tits, J., Dardenne, K., Liu, X., Rothe, J., Denecke, M.A., Wieland, E., Altmaier, M., 2012. Spectroscopic investigations of Np(V/VI) redox speciation in hyperalkaline TMA-(OH, Cl) solutions. Radiochim. Acta 100, 759–770.

Gayer, K.H., Leider, H., 1957. The solubility of uranium(IV) hydroxide in solutions of sodium hydroxide and perchloric acid at 25 °C. Can. J. Chem. 35, 5–7.

Grambow, B., Smailos, E., Geckeis, H., Müller, R., Hentschel, H., 1996. Sorption and reduction of uranium(VI) on iron corrosion products under reducing saline conditions. Radiochim. Acta 74, 149–154.

Grenthe, I., Fuger, J., Konings, R.J.M., J, L.R., Müller, A.B., Nguyen-Trung, C., Wanner, H., 1992. Chemical Thermodynamics of Uranium, Vol. 1 of Chemical Thermodynamics. Elseiver Science Publishers, Amsterdam.

Guillaumont, R., Fanghänel, T., Fuger, J., Grenthe, I., Neck, V., Palmer, D.A., Rand, M.H., 2003. Update on the Chemical Thermodynamics of Uranium, Neptunium, Plutonium, Americium and Technetium, Vol. 5 of Chemical Thermodynamics. Elseiver Science Publishers, Amsterdam.

Hennig, C., Ikeda-Ohno, A., Emmerling, F., Kraus, W., Bernhard, G., 2010. Comparative investigation of the solution species $[U(CO_3)_5]^{6-}$ and the crystal structure of $Na_6[U(CO_3)_5]{\cdot}12H_2O$. Dalton Trans. 39, 3744–3750.

Hennig, C., Ikeda-Ohno, A., Tsushima, S., Scheinost, A.C., 2009. The Sulfate coordination of Np(IV), Np(V), and Np(VI) in aqueous solution. Inorg. Chem. 48, 5350–5360.

Huber, F., Schild, D., Vitova, T., Rothe, J., Kirsch, R., Schäfer, T., 2012. U(VI) removal kinetics in presence of synthetic magnetite nanoparticles. Geochem. Cosmochim. Acta 96, 154–173.

Hummel, W., Anderegg, G., Puigdomènech, I., Rao, l., Tochiyama, O., 2005. Chemical Thermodynamics of U, Np, U, an, Tc, Se, Ni and Zr with Selected Organic Ligands, Vol. 9 of Chemical Thermodynamics. Elseiver Science Publishers, Amsterdam.

Ilton, E.S., Boily, J.F., Buck, E.C., Skomurski, F.N., Rosso, K.M., Cahill, C.L., Bargar, J.R., Felmy, A.R., 2010. Influence of dynamical conditions on the reduction of U^{VI} at the magnetite-solution interface. Environ. Sci. Technol. 44, 170–176.

Kim, J.I., Grambow, B., 1999. Geochemical assessment of actinide isolation in a German salt repository environment. Eng. Geol. 52, 221–230.

Kobayashi, T., Scheinost, A.C., Fellhauer, D., Gaona, X., Altmaier, M., 2013. Redox behavior of Tc(VII)/Tc(IV) under various reducing conditions in 0.1 M NaCl solutions. Radiochim. Acta 101, 323–332.

Latta, D.E., Gorski, C.A., Boyanov, M.I., O'Loughlin, E.J., Kemner, K.M., Scherer, M.M., 2012. Influence of magnetite Stoichiometry on U^{VI} reduction. Environ. Sci. Technol. 46, 778–786.

Lefevre, G., Kneppers, J., Fédoroff, M., 2008. Sorption of uranyl ions on titanium oxide studied by ATR-IR spectroscopy. J. Colloid Interface Sci. 327, 15–20.

Lemire, R.J., Fuger, J., Spahiu, K., Nitsche, H., Sullivan, J.C., Potter, P., Ullmann, W.J., Rand, M.H., Rydberg, J., Vitorge, P., H, W., 2001. Chemical Thermodynamics of Neptunium and Plutonium, Vol. 4 of Chemical Thermodynamics. Elseiver Science Publishers, Amsterdam.

Liger, E., Charlet, L., Van Cappellen, P., 1999a. Surface catalysis of uranium(VI) reduction by iron(II). Geochem. Cosmochim. Acta 63, 2939–2955.

Liger, E., Charlet, L., Van Cappellen, P., 1999b. Surface catalysis of uranium(VI) reduction by iron(II). Geochem. Cosmochim. Acta 63, 2939–2955.

Metz, V., Geckeis, H., González-Robles, E., Loida, A., Bube, C., Kienzler, B., 2012. Radionuclide behaviour in the near-field of a geological repository for spent nuclear fuel. Radiochim. Acta 100, 699–713.

Metz, V., Kienzler, B., Schüßler, W., 2003. Geochemical evaluation of different groundwater-host rock systems for radioactive waste disposal. J. Contam. Hydrol. 61, 265–279.

Missana, T., Maffiotte, U., García-Gutiérrez, M., 2003. Surface reactions kinetics between nanocrystalline magnetite and uranyl. J. Colloid Interface Sci. 261, 154–160.

Morel, M.M.F., Hering, J.G., 1996. Principals and Applications of Aquatic Chemistry. John Wiley & Sons, New York.

Neck, V., Kim, J.I., 2001. Solubility and hydrolysis of tetravalent actinides. Radiochim. Acta 89, 1–16.

O'Loughlin, E.J., Kelly, S.D., Cook, R.E., Csencsits, R., Kemner, K.M., 2003. Reduction of uranium(VI) by mixed iron(ii)/iron(iii) hydroxide (green rust): formation of UO_2 nanoparticies. Environ. Sci. Technol. 37, 721–727.

Parks, G.A., Pohl, D.C., 1988. Hydrothermal solubility of uraninite. Geochem. Cosmochim. Acta 52, 863–875.

Puigdoméènech, P., 1983. INPUT, SED and PREDOM: Computer Programs Drawing Equilibrium Diagrams, TRITA-ook-3010. Royal Institute of Technology (KTH), Dept. Inorg. Chemistry, Stockholm (Sweden).

Rai, D., Felmy, A.R., Ryan, J.L., 1990. Uranium(IV) hydrolysis constants and solubility product of $UO_2{\cdot}xH_2O$(am). Inorg. Chem. 29, 260–264.

Ravel, B., Newville, M., 2005. ATHENA, ARTEMIS, HEPHAESTUS: data analysis for X-ray absorption spectroscopy using IFEFFIT. J. Synchrotron Radiat 12, 537–541.

Rothe, J., Butorin, S., Dardenne, K., Denecke, M.A., Kienzler, B., Loble, M., Metz, V., Seibert, A., Steppert, M., Vitova, T., Walther, C., Geckeis, H., 2012. The INE-Beamline for actinide science at ANKA. Rev. Sci. Instrum. 83.

Rovira, M., El Aamrani, S., Duro, L., Giménez, J., de Pablo, J., Bruno, J., 2007. Interaction of uranium with in situ anoxically generated magnetite on steel. J. Hazard Mater. 147, 726–731.

Ryan, J.L., Rai, D., 1983. The solubility of uranium(IV) hydrous oxide in sodium-hydroxide solutions under reducing conditions. Polyhedron 2, 947–952.
Schmidt, J., Vogelsberger, W., 2009. Aqueous long-term solubility of Titania nanoparticles and titanium(iv) hydrolysis in a sodium chloride system studied by adsorptive Stripping voltammetry. J. Solut. Chem. 38, 1267–1282.
Schwertmann, U., Cornell, R.M., 2000. Iron Oxides in the Laboratory: Preparation and Characterization. Wiley-VCH, Weinheim, New York.
Scott, T.B., Allen, G.C., Heard, P.J., Randell, M.G., 2005. Reduction of U(VI) to U(IV) on the surface of magnetite. Geochem. Cosmochim. Acta 69, 5639–5646.
Spahiu, K., Devoy, J., Cui, D.Q., Lundstrom, M., 2004. The reduction of U(VI) by near field hydrogen in the presence of UO_2(s). Radiochim. Acta 92, 597–601.
Spahiu, K., Werme, L., Eklund, U.B., 2000. The influence of near field hydrogen on actinide solubilities and spent fuel leaching. Radiochim. Acta 88, 507–511.
Stumm, W., Morgan, J.J., 1996. Aquatic Chemistry, third ed. John Wiley & Sons, New York.
Sullivan, J.C., Cohen, D., Hindman, J.C., 1957. Kinetics of reactions involving neptunium (iv), Neptunium(V) and neptunium(VI) ions in Sulfate media. J. Am. Chem. Soc. 79, 4029–4034.
Tan, T.T.Y., Beydoun, D., Amal, R., 2003. Photocatalytic reduction of Se(VI) in aqueous solutions in UV/TiO_2 system: kinetic modeling and reaction mechanism. J. Phys. Chem. B 107, 4296–4303.
Tits, J., Gaona, X., Laube, A., Wieland, E., 2014. Influence of the redox state on the neptunium sorption under alkaline conditions: batch sorption studies on titanium dioxide and calcium silicate hydrates. Radiochim. Acta 102, 385–400.
Tremaine, P.R., Chen, J.D., Wallace, G.J., Boivin, W.A., 1981. Solubility of uranium (iv) oxide in alkaline aqueous-solutions to 300 °C. J. Solut. Chem. 10, 221–230.
Wehrli, B., Sulzberger, B., Stumm, W., 1989. Redox processes catalyzed by hydrous oxide surfaces. Chem. Geol. 78, 167–179.
Wieland, E., Van Loon, L.R., 2002. Cementitious Near-field Sorption Data Base for Performance Assessment of an ILW Repository in Opalinus Clay. Nagra Technical Report NTB 02–20. Nagra, Wettingen. Switzerland.
Yalcintas, E., Gaona, X., Scheinost, A.C., Kobayashi, T., Altmaier, M., Geckeis, H., 2015. Redox chemistry of Tc(VII)/Tc(IV) in dilute to concentrated NaCl and $MgCl_2$ solutions. Radiochim. Acta 103, 57–72.
Yan, S., Chen, Y.H., Xiang, W., Bao, Z.Y., Liu, C.X., Deng, B.L., 2014. Uranium(VI) reduction by nanoscale zero-valent iron in anoxic batch systems: the role of Fe(II) and Fe(III). Chemosphere 117, 625–630.
Zhao, R., Wang, L., Gu, Z.J., Yuan, L.Y., Xiao, C.L., Zhao, Y.L., Chai, Z.F., Shi, W.Q., 2014. A facile additive-free method for tunable fabrication of UO_2 and U_3O_8 nanoparticles in aqueous solution. CrystEngComm 16, 2645–2651.
Zimina, A., Dardenne, K., Denecke, M.A., Huttel, E., Lichtenberg, H., Mangold, S., Prüßmann, T., Rothe, J., Spangenberg, T., Steininger, R., Vitova, T., Geckeis, H., Grunwaldt, J.-D., 2017. CAT-ACT a new highly versatile X-ray spectroscopy beamline for catalysis and radionuclide science at the KIT synchrotron light facility ANKA. Rev. Sci. Instrum. 88, 113113.